The Thesis Committee for Genesok Oh
Certifies that this is the approved version of the following thesis:

The Effect of Crude Oil and Chemical Dispersant on Sinking Rates of Gulf of Mexico Diatoms

APPROVED BY
SUPERVISING COMMITTEE:

Supervisor:

Tracy A. Villareal

Edward J. Buskey

Zhanfei Liu

The Effect of Crude Oil and Chemical Dispersant on Sinking Rates of Gulf of Mexico Diatoms

by
Genesok Oh, B.S.

Thesis

Presented to the Faculty of the Graduate School of

The University of Texas at Austin

in Partial Fulfillment

of the Requirements

for the Degree of

Master of Science in Marine Science

The University of Texas at Austin
December 2015

Dedication

This thesis is dedicated to Seiwoong, Sunmi, and Joon for always giving their support and encouragement.

Acknowledgements

I would like to thank my advisor, Dr. Tracy A. Villareal, for his guidance during my past two years at the University of Texas Marine Science Institute. A special thanks also goes to my committee members, Dr. Edward J. Buskey and Dr. Zhanfei Liu for their helpful insight and feedback to my thesis project.

I would like to thank Dr. Brad Gemmell for his help in understanding and setting up the optical filming system. A thank you goes to Cammie Hyatt for her help acquiring oil and dispersant. Thanks also go to Dr. Bryan Black for his statistical consultation.

A special thanks goes to Matt Seeley, Matt Dzaugis, Carrie Harris, and Meredith Evans, who made graduate school a very enjoyable experience, I could not have asked for a better cohort and friends.

Thank you to my family, who have loved and supported me through this endeavor. Thank you to my brother, Joon for being my lifelong best friend. And Mom and Dad, for always supporting my interests even when they were strange, showing me the success of hard work by example, and being a great compass for me in life.

Abstract

The Effect of Crude Oil and Chemical Dispersant on Sinking in Gulf of Mexico Diatoms

Genesok Oh, M.S. MarineSci

The University of Texas at Austin, 2015

Supervisor: Tracy A. Villareal

In the open and coastal ocean, primary productivity is derived largely from phytoplankton. Diatoms are a major group of phytoplankton that account for almost half of all oceanic primary production. Sinking is a fundamental aspect of diatom ecology usually linked to loss process but is important in vertical migration for nutrient uptake, avoidance of predators, and completion of lifecycle events. Sinking is tightly linked to both physiological state and size of diatom cells. Oil spills are one of the many stressors now evident in the marine environment. Since diatom physiology is generally adversely affected by crude oil in the form of growth inhibition, reduced photosynthesis, and cell death, it was hypothesized that diatom sinking would be adversely affected by the addition of crude oil, and that increasing concentration, time, and the addition of chemical dispersant would magnify this effect. There has been no previous study attempting to quantify how diatom sinking is affected by the presence of crude oil and

chemical dispersant. In this study, laboratory cultures of diatom species were experimentally treated with crude oil, dispersant, and a mixture that was filmed at three timepoints over the course of a week. Images were processed with ImageJ to quantify individual trajectories. There were 20-50 cells examined per treatment, with a goal of 50 observed cells. Killed cells showed higher average sinking rates (*C. wailesii*=93.7 ± 32.9 m day^{-1}, *H. cuneformis*= 22.9 ± 5.37 m day^{-1}) than the highest observed treatment (*C. wailesii*=65.9 ± 26.9 m day^{-1}, *H. cuneformis*=20 ± 5.66 m day^{-1}). There was no clear trend of increased mean sinking rate with respect to treatment or time. Clear dose-response curves for sinking were not evident. Skewness and kurtosis was calculated for each treatment to examine changes in the frequency distributions of sinking rate histograms, and compared to the controls to observe any patterns of change in central tendency or kurtosis. There was no trend with respect to skewness or kurtosis, although the data suggests there may be species-specific differences in response in *H. cuneformis* and *Skeletonema spp.* treatments, where one side of the skewness axis was favored. The data suggests that exposure to crude oil and chemical dispersant does not elicit a clear increase in sinking rate. If these results can be generalized to the field, then diatom population changes after an oil spill is likely not due to major changes in sinking losses.

Table of Contents

List of Tables

List of Figures

Introduction

Carbon production by marine phytoplankton, the basis of most marine food webs, is estimated at 43.5 Pg C yr^{-1} (Behrenfeld & Falkowski 1997). With an estimated 200,000 different species, diatoms are a diverse group of phytoplankton ranging in size from micrometers to millimeters as single cells or connected chains (Kooistra 2007, Villareal 1991) and account for roughly 40% of oceanic primary production (Falkowski & Raven 2007, Hopkinson et al. 2011. These eukaryotic phytoplankton tend to dominate coastal and upwelling regions, as well as the sea-ice border, which are areas with sufficient light, nitrogen, phosphorus, silicon, and trace elements for sustained growth (Armbrust 2009). Diatoms form blooms that are major sources of "new" production and carbon sedimentation globally (Burrell 1988). Due to their characteristic silica frustule, diatoms can be relatively dense and are capable of very rapid sinking (Walsby & Reynolds 1980).

DIATOM SINKING

Sinking is both a loss factor as well as an important ecological strategy for diatoms (Fig. 1). It enables vertical migration for nutrient uptake, completion of life cycle events, and avoidance of grazing pressure by visual predators (Smetacek 1985). It is also of biogeochemical importance, as diatom sinking is a major factor in the removal of CO_2 from the atmosphere to the deep sea through the biological pump (Ragueneau et al. 2000). The rate of oceanic carbon export is primarily

governed by the sinking speed of dead diatom cells and aggregates, along with fecal pellets (Ragueneau et al. 2000). Rapid sinking is due mainly to physical aggregation of phytoplankton cells from excretion of exopolymeric substances (EPS) that then slough off cell walls to form larger gel aggregates called transparent exopolymeric particles (TEP). These TEP particles are a major contributor to marine snow (Passow 2000, Passow et al. 2012). Individual cell sinking rates are often invoked in understanding successional patterns and the relationship of diatoms to turbulence (Margalef 1978, Smayda & Reynolds 2001). Phytoplankton sinking can also influence the cycling and transport of metals and chemical constituents in the ocean, making them of interest to sedimentologists (Bienfang 1981, Fisher & Wente 1993, Margalef 1978, Smayda & Reynolds 2001). Thus, it is of vital interest to understand sinking characteristics of diatoms for the vertical distribution of phytoplankton biomass and oceanic carbon sequestering (Smayda 1970).

Sinking rates of marine phytoplankton are a function of physical factors such as cell size and shape; sinking rate increases with both cell size and density (Smayda 1970). For solitary cells, calculations show a 10-fold increase in cell diameter equates to a 15 to 20-fold increase in sinking speeds of healthy and senescent populations (Smayda 1970). However, theoretical calculations of diatom sinking speeds have shown disparity with empirical observations (Miklasz & Denny 2010, Smayda 1970, Waite et al. 1997). That is, larger cells do not sink as fast as expected based on merely their size and morphology.

Photosynthetic rate, and thus primary production, is dependent on the residence time within the euphotic zone (>1% light); however, continuous residence in the euphotic zone is not required (Smayda 1970, 1971). Physiological factors, such as buoyancy regulation through carbohydrate ballasting and exchange of intracellular ions (ex. NH_4^+ over SO_4^{2-}), play a role in slowing sinking rates of some phytoplankton cells out of the photic zone at the cost of steady energy expenditure (Gross & Zeuthen 1948, Smayda 1970, Villareal & Carpenter 1990, Villareal & Carpenter 2003). Breakdown of cellular ion gradients upon death of the cell or under metabolic stress also result in a slightly increased sinking rate (Eppley et al. 1967, Waite et al. 1992).

Maintenance of the internal gradients necessary for buoyancy control requires energy and links sinking rate to phytoplankton physiological state (Anderson & Sweeney 1977, Eppley et al. 1967, Smayda 1970, Waite et al. 1992). Nutrient limitation though silicate and phosphate depletion increased sinking rate in diatoms and phytoplankton assemblages (Bienfang et al. 1982, Bienfang & Harrison 1984). Sinking is also an ecological strategy for nutrient uptake and sinking rates decrease once sinking cells are immersed in higher nutrient concentrations (Bienfang et al. 1983). A faster sinking rate will also shrink the boundary layer, allowing more rapid diffusion of nutrients to the cell surface (Gavis 1976, Munk & Riley 1952). In *Ditylum brightwellii*, smaller cells sank faster than larger cells under saturating light, but under severe light limitation the sinking rate was based on cell size (Waite et al. 1992). However, the effects of light on sinking are not as clear-cut as nutrient

deprivation. Other studies show that the relationship of irradiance to sinking rates varies (Bienfang 1980, Culver & Smith 1989, Granata 1991, Johnson & Smith 1986). It is only when the diatom cell reaches a severe physiologically taxed or dead state that sinking speeds asymptotically approach a maximum size dependent sinking speed calculated by Stokes' law (Smayda 1970, Waite et al. 1992; text Figure 2). Turbulence can also increase the average sinking speeds of phytoplankton cells by physical processes (Ruiz et al. 2004). Other methods of accelerated sinking include density inversion currents, aggregation of cells, downwelling, and descent in fecal pellets (Smayda 1971).

Diatom cells have three states of sinking rates: neutrally buoyant, logarithmic growth, and non-growing (text Table 1, Figure 3; Eppley et al. 1967, Smayda 1971). For example with *D. brightwellii*, non-growing populations had a significantly higher sinking rate than growing cultures, and there were very slow sinking to neutrally buoyant cells present (Eppley et al. 1967). Histograms are a useful tool to visual the shape of the distribution; Shifts in average sinking rate would represent shifting modes on the individual sinking rate frequency distribution of a given population.

SINKING RATE MEASUREMENTS

It is a challenge to measure phytoplankton sinking rates *in-situ*, due to ocean convection and micro-scale turbulence. Visual sinking rate measurements of these patches are generally crude and inaccurate. The most common form of measuring sinking rates involves the use of settling columns (SETCOL) initially containing a

uniform mixture of a cell population, and calculating the sinking rate based on changes in the vertical distribution over time (Bienfang 1981). Another method is the use of a fluorometer by measuring decreases in chlorophyll fluorescence though a column window (Eppley et al. 1967). A continuous laser scanning method coupled with a vertical Percoll density gradient is likely the most accurate method of measuring phytoplankton sinking rates, but cannot distinguish different cells types or species, or parse out individual cell sinking rates (Walsby & Holland 2006). For individual particle sinking rates, there is a new methodology of filming individual particles as they sink through a stable salinity density gradient (O'Brien et al. 2006). This method has higher reported sinking rates than the SETCOL method (Fig. 4) on the same cultures.

CRUDE OIL IN THE ENVIRONMENT

Oil is a physiological stressor that impairs some physiological functions in many species of phytoplankton (Harrison et al. 1986, Ozhan & Bargu 2014a&b, Ozhan et al. 2014a&b). As noted above, diatom cells reaching a severe physiologically taxed or dead state will show an increase in sinking speed (Waite et al. 1992). Therefore, it is reasonable to consider the impact of oil spills on sinking losses of diatoms as a potential additional loss factor. Among crude oil consituents, polycyclic aromatic hydrocarbons (PAHs) are some of the most toxic components. There are many sources of PAHs to the environment, including pipeline spills, natural seeps of crude oil, operational discharges, and tanker and platform accidents

(Ozhan et al. 2014b). Of these, accidental spills by tankers and platforms cause major concern due to the acute exposure of high concentration PAHs they cause to biological communities around the spill (Gilde & Pinckney 2012). Marine oil spills have many complex interactions within a water column as highlighted by Figure 5 (McGenity et al. 2012). Increases in oil spills in the last century, along with a growing human population and demand for energy, highlight that the presence of large amounts of PAHs in marine waters is likely to continue on this upward trend. From 1910 to 1961, there was an average of 1.24 ±0.43 occurrences spilling 114,062 ± 352,512 tons of oil per year (Morgan et al. 2014). From 1991 to 2012, this increased to 6.50 ± 5.17 spills with 164,299 ± 290,655 tons of oil spilt per year. Acute pollution events can cause mass mortality, such as in the Prestige spill where over 66% of total species richness was lost in the most heavily impacted beaches (de la Huz et al. 2005). As marine environments become more exposed to PAHs, it is increasingly more important to understand how it can affect these organisms that are a vital base component to freshwater and marine ecosystems.

DEEPWATER HORIZON

The Deepwater Horizon oil spill, one of the largest marine oil spills to date, constituted a major environmental perturbation to the Gulf of Mexico (GoM) phytoplankton community. It occurred from April 20th to July 15th in 2010 and leaked an estimated 4.16 to 6.24 million barrels of Louisiana sweet crude (LSC) oil into the Gulf of Mexico (Crone & Tolstoy 2010), an area responsible for around 25%

of the nation's seafood landings (Adams et al. 2004). This resulted in large, cohesive mats of oil on the surface due to the oil's relatively low density and a unique opportunity to assess ecosystem effects of such a large perturbation. Surface oil slicks can limit gas exchange at the air-sea interface and limit phytoplankton photosynthesis by reducing light penetration up to 90% (Nelson-Smith 1973, Gonzalez et al. 2009). However, the complexity of interactions is difficult to untangle, as temporary stimulation of phytoplankton growth following the spill was suggested by remote sensing analyses (MODIS fluorescence line height data analysis; Hu et al. 2011). There may have also been stimulation of marine snow production shortly after the Deepwater Horizon oil spill, where large mucus-rich marine snow mats formed (Passow et al. 2012). These were products of mucous webs of bacterial oil degraders, interactions of oil and particulate matter, and coagulation of phytoplankton with oil droplets as illustrated in Figure 6. Spilled oil is thought to reach the benthos mainly by marine snow formation in oil-contaminated surface waters (Oil Budget Calculator Science and Engineering Team 2010, Patton et al. 1981). One of the methods used to mitigate the environmental impacts of the spill was the spray addition of ~1.8 to 6 million gallons of chemical dispersant, mainly Corexit EC9500A (Judson et al. 2010, Ozhan & Bargu 2014b). While the application of dispersant at the wellhead later in the spill reduced the amount of oil that reached the ocean surface and potentially mitigated some of its impacts to coastal wetlands and shorelines around the GoM, the dispersed oil introduced a large amount of hydrocarbons into the water column.

DIATOMS AND CRUDE OIL

Phytoplankton community responses to crude oil and dispersants using both monocultures and natural communities have indicated that crude oil composition and solubility determines the toxicity effect (Glide & Pinckney 2012, Gordon et al. 1973, Liu et al. 2006, Ozhan & Bargu 2014a & b, Ozhan et al. 2014a). A confounding factor in exposure studies is the change in particulate oil concentrations over time and with differing light intensity (Fig. 7). Different types of crude oil elicit different responses in marine phytoplankton (Table 2). Volatile aromatics, such as naphthalene and benzene, are the most toxic of the water-soluble components of oil (Kusk 1978). Along with this, phytoplankton response to crude oil is also dependent on natural parameters such as phytoplankton species, temperature, nutrients, and light intensity; the 50% effective concentration for cell death (EC50; Table 2) varies among species from 1 mg L^{-1} to >50 mg L^{-1} (Harrison et al. 1986). Due to the complex interactions of seawater and crude oil, Water-accommodated fractions (WAFs) are more suitable for phytoplankton physiological studies than oil emulsions, as the WAF technique reduces oil-particle interactions. In sinking studies, oil-particle interactions can cause modification in diatom sinking rates by adherence to the frustule, changing the density and shape of the particle.

Temperature increases lead to increased growth rate and subsequently metabolic rate, which increases toxicant absorption and consequently toxicity (Huang et al. 2011). Data suggests centric diatoms are more sensitive to oil and dispersant mixtures than microflagellates and dinoflagellates (Harrison et al. 1986).

Diatom size may also play a role in determining toxic effect, although there is conflicting data on this. Ozhan et al. (2014b) tested South Lousiana sweet crude (LSC) oil toxicity on five GoM phytoplankton species and found larger species to be more tolerant to crude oil, while Gonzales et al. (2009) found opposing results.

PHYSIOLOGICAL RESPONSE TO CRUDE OIL AND DISPERSANT

Diatom physiology is adversely affected by crude oil, but there is not a simple yield-dose relationship. At lower concentrations of oil (ex. 1 mg/liter), diatom growth is slightly stimulated (Dunstan et al. 1975), while higher concentrations showed a strong level of growth inhibition (Harrison et al. 1986, Hsiao et al. 1978, Lee et al. 1977, Parson et al. 1976, Pulich et al. 1974). Aromatic hydrocarbons in crude oil up to 700 mg benzene L^{-1} have been shown to reduce photosynthesis rates in *Nitzschia palea.* At higher concentration, photosynthesis was irreversibly halted (Kusk 1978).

Crude oil and dispersants coupled together can be more toxic to some diatom growth rates than either individually as shown in Figure 8 (Harrison et al. 1986, Hook & Osborn 2012, Jung et al. 2012, Ozhan et al. 2014a). This enhanced physiological stress implies diminished physiological cell state that may alter increase cell sinking. Ozhan and Bargu (2014b) noted that the phytoplankton community's growth sensitivity to Louisiana sweet crude oil (LSC) correlates with PAH concentration and nutrient stress; the greater the nutrient deficit, the more inhibitory effect that LSC had (Fig. 9). Diatoms show an enhanced sensitivity to oil

and dispersant mixtures relative to dinoflagellates and microflagellates (Hook & Osborn 2012, Sikkema et al. 1995) with greater growth inhibition and membrane damage at comparable concentrations relative to other phytoplankton species .The addition of the chemical dispersant Corexit EC9500A alone and in combination with LSC also showed a strong inhibitory effect on growth in some phytoplankton (Hook & Osborn 2012, Ozhan & Bargu 2014b). Prudhoe Bay crude oil and Corexit 9527 separately do not inhibit phytoplankton growth, but together they create a greater effect of growth inhibition (Parsons et al. 1976, Parsons et al. 1984). The only study that examined diatom sinking rates with oil and dispersant exposure were mesocosm studies (Harrison et al. 1986) that noted increases in sinking rate that coincided with nutrient exhaustion and but were not affected solely by oil or Corexit exposure (Fig. 10).

SUMMARY

The general trend is that declining cell state leads to an increase in phytoplankton sinking rates. Crude oil and dispersant mixtures are physiological stressors in multiple ways to many species of phytoplankton. Crude oil at a concentration that causes sub-lethal effects will likely elicit a negative physiological response. Therefore, it is hypothesized that exposure to crude oil will result in higher sinking velocities in most species of diatoms. It is also hypothesized that addition of chemical dispersant will increase oil toxicity and thus sinking rates. Quantification of sinking speed change in diatoms with crude oil and dispersant

exposure would allow us to infer if loss through sinking is another added effect of acute oil exposure.

Methods

CELL ISOLATION

Water samples were collected by plankton net tows (20 μm mesh size, 28 cm diameter) conducted in surface waters off the UTMSI ship channel pier. Sampling lasted two minutes and coincided with incoming tidal movement to capture coastal species of diatoms.

Qualitative light microscopy analysis using an Olympus BZH light microscope (6 v, 20 w) was used to identify the phytoplankton community. Individual cells were picked out by isolation pipette. Sequential rinses through a 9-well depression plate containing sterile medium was done multiple times to ensure a unialgal culture. Between each use, the mouth pipette was immersed in milli-Q® water maintained above 60° C to eliminate contamination. Each cell was initially placed into a glass test tube with 20-30 mL of sterile media (MET-44) until growth was observed, and then transferred to 250 mL polystryene culturing flasks for propagation (Schöne & Schöne 1982). *Coscinodiscus wailesii* (isolated 1/3/2015, average size 8,140,000 μm^3, standard deviation ± 1,520,000 μm^3), *Pseudosolenia calcar-avis* (isolated 8/21/2015, avg 41,000 μm^3, sd ± 9,100 μm^3), *Skeletonema spp.* (isolated 9/13/2015, avg 15,000 μm^3, sd ± 2,400 μm^3), and *Hemidiscus cuneiformis* (isolated 10/1/2015, avg 4,520,000 μm^3, sd ± 910,000 μm^3) are the species used in this study (Fig. 11). These averages were generated from 30 random cells in the initial control population; the standard deviation is ~20% of each average. *C.wailesii, P.calcar-avis,* and *Skeletonema spp.* are a cylindrical shape and cell volume was calculated with $V=\pi r^2 h$; *H.cuneformis* is a wedge shaped and measured to be roughly a

quarter of a sphere, so cell volume was calculated by $V=(^4/_3\pi r^3)/4$. Cell dimensions were measured through Image-J.

MEDIA PREPARATION

Seawater was collected from the UTMSI flowing seawater system and filtered through a 47mm glass fiber/f (GF/F) filter. After MET-44 (Schöne and Schöne 1982) nutrient addition, media was filtered through Nalgene rapid flow sterile filtration before use in cultures.

CELL CULTURING

Successful phytoplankton monocultures of *C. wailesii, Pseudosolenia calcar-avis, Skeletonema spp., Hemidiscus cuneformis* were placed in walk-in incubators maintained at 20-23°C on 12:12 light/dark cycles. The cells were grown in a constant light level of 136.12 μE $m^{-2}sec^{-1}$, which was measured using a Lab Quantum Scalar Irradiance Meter. Growth media in the cultures was diluted every five days to insure exponential growth phases.

EXPERIMENTAL TREATMENT TO CRUDE OIL

After ~ 2 weeks of growth, cells were exposed to LSC oil (Source oil from Marlin Platform Dorado collected 2/1/2012) prepared with a water-accommodated fraction (WAF) technique that was prepared according to the method described in The Chemical Response to Oil Spills: Ecological Research Forum (CROSERF) (Aurand & Coelho

2005, Ozhan and Bargu 2014b). WAF was prepared with filtered (0.7 μm) and autoclaved GoM seawater (Salinity:32-35) in 1-L Pyrex, valved-outlet glass bottles. The oil (200 g) was added by weight difference with a gas-tight Hamilton© syringe into 800 mL of seawater and mixed at a stirring rate of 140-160 rpm with a 1-inch stir bar (Figure 12). The chemically enhanced water-accommodated fraction (CEWAF) was prepared in the same method at a higher mixing rate (~650 rpm), with an addition of chemical dispersant COREXIT 9500a at a 1:100 oil:dispersant ratio. After 24 hours of mixing, both mixtures were settled for 4 hours and drawn out through a valve on the bottom of the bottle to avoid disturbing the oil-water interface before immediate use in treatments. 50 mL samples for chemical analysis were collected in amber glass jars and stored at 4°C. The lower concentrations for each treatment below were used in our first experiment with *C.wailesii*. No significant effect on sinking rates was observed, and increased oil concentrations were used in subsequent experiments. There were seven treatments of 350 mL in separate 500 mL glass Erlenmeyer flasks:

1. Control flask with no addition
2. Low WAF (2.5-10 ppm Total petroleum hydrocarbon (TPH))
3. High WAF (10-100 ppm)
4. Low Dispersant (0.125-0.5 ppm)
5. High Dispersant (0.5-5 ppm)
6. Low CEWAF (2.5-10 ppm TPH + 1:100 ratio of Corexit 9500A)
7. High CEWAF (10-100 ppm TPH + 1:100 ratio of Corexit 9500A).

These concentrations are values used and shown to have sub-lethal effects on phytoplankton (Hook and Osborn 2014, Harrison et al. 1986, Ozhan and Bargu 2014b). The estimated lower range of concentrations was used for *C. wailesii* and when no effect was observed we used the estimated higher end of concentrations for the subsequent species. Experimental treatments were compared to heat killed controls (60°C) for *C. wailesii* and *H. cuneformis*. *P. calcar-avis* and *Skeletonema spp.* did not have a heat killed treatment as the cultures died after the experimental treatments but before the heat killed control experiment.

STABLE HALOCLINE FORMATION

Individual particle tracking was used to measure cell sinking rates. This requires a stable water column to accurately measure speeds without convection as a factor. The stable water column was established by a salinity gradient (O' Brien et al. 2006) where filtered seawater was pumped by a Carter 4/8 cassette pump (Item number 72-320-048) into two chambers (Tube diameter: 0.15 mm) (O'Brien et al. 2006). There was a high (~35 psu) salinity chamber connected to a low (~27 psu) salinity chamber with a mixing bar. Seawater was pumped into a plexi-glass column (5.7 cm x 6.5 cm x 20.5 cm, 700 ml seawater volume) from the lower salinity chamber that became increasingly more saline and dense as the removed water was replaced by water from the higher salinity chamber (Fig. 13). This two-tank method for creating a stable density gradient is explained in further detail by Hill (2002).

The resulting water column is a continuous salinity gradient with a 2 psu difference from the top and bottom (27-29 psu), which was measured by taking seawater aliquots from the top, middle, and bottom of the column. The experimental room was kept at a constant temperature (24°C). Filming of injected dye in tests shows that there was no convection or mixing of layers of seawater over the course of several days. Density gradients may introduce a problem in measurement as the sinking cell encounters increasing viscosity and density (Walsby & Holland 2006); however, our salinity differences within our filming window only results in a calculated change in water density of 0.0001 kg/m^3 (997.347 kg/m^3 to 997.3471 kg/m^3), assuming constant pressure (1 atm) and temperature (24°C).

FILMING

Cells were either added to the top of the column by pipette or gently added to the low salinity chamber during mixing, depending on size (Fig. 14) and filmed using a Nikon D7100 camera with 68mm extension rings and an af-s micro-Nikkor 105 mm lens (aperture f/ 2.8) at a rate of 24 frames per second. A light source (175 w) was placed 45 cm away from the column pointed at the middle of the column (Fig. 13). The filming window was 1.8 cm x 1.9 cm, with a focus depth of 2.6 cm near the middle of the column, with clearance to wall of ~3 cm. Initial experiments with *C. wailesii* were conducted at 1, 6, and 24 hour points. Subsequent experiments were sampled at over a 7-day time series at one hour, one day, and one week time points after the initial experiments indicated no acute effects were observed at 24 hours.

DATA ANALYSIS

Videos were roughly 8 minutes in length, with the objective to capture 50 cells per treatment. Videos (.mov format) were converted to image sequences (.tiff format) using Quicktime Pro, and then analyzed through freeware Image-J, with a 2D particle tracking MOSAIC plug-in (Sbalzarini & Koumoutsakos 2005). This allowed tracking of individual particle sinking rates; cells in focus were visually chosen to ensure cells near walls potentially experiencing drag effects were not measured (Brenner 1962). A frame of an image sequence of *H. cuneformis* (Fig. 15) is presented as an example. Trajectories were then quantified in MS Excel based on how many pixels the cell traveled per second. Histograms were constructed from each individual diatom particle sinking rates using the average velocity (m sec^{-1}) to show the sinking distributions in a given treatment.

Means and medians were recorded for each treatment to observe any trends over time and treatment level. A chi-squared analysis was used to determine if there were significant differences between distributions of each experimental treatment and the control for that time point. Using open source statistical software R, the skewness and kurtosis of each treatment was calculated and compared to visualize any changes in central tendency or kurtosis. The skewness represents the lack of symmetry in the distribution, and the kurtosis is the tightness and height of the distribution peak.

Results

POPULATION SINKING CHARACTERISTICS

The cell volume of the four species was calculated from measurements of 30 cells for each species (Fig. 16). *C. wailesii* (8,140,000 μm^3) had a larger cell volume than any other species, followed by *H. cuneformis* (4,500,000 μm^3), *P. calcar-avis* (41,000 μm^3), then *Skeletonema spp.* (15,000 μm^3). *C. wailesii,* and *H. cuneformis* are solitary cells, and *P. calcar-avis* was also recorded as single cells due to weak chain linkages that often broke during filming. *Skeletonema spp.* is a chain-forming diatom and averaged short 4-6 cell chains in our recordings. Cell sizes were consistent, each species had a ~20% average deviation in cell size. *C. wailesii, P. calcar-avis,* and *Skeletonema spp.* are cylindrically shaped, although *C. wailesii* has a much greater radius. *H. cuneformis* is a wedge shaped diatom.

Sinking speeds of a heat-killed population was quantified for *C. wailesii* and *H. cuneformis* (Fig. 17). This represented the maximum sinking velocity that a cell of that size, as dead cells would sink solely based on the physical factors of cell size and shape at that density (Smayda 1974). The average sinking speed of the heat killed treatments (Fig. 17) for *C. wailesii* (n=30, 93.7 ± 32.9 m d^{-1}) and *H. cuneformis* (n=50, 22.9 ± 5.37 m d^{-1}) was higher than the maximum speeds reached in any experimental treatment show in Figure 19 (*C. wailesii*=65.9 ± 26.9 m d^{-1}, *H. cuneformis*=20 ± 5.66 m d^{-1}).

The sinking speed ranges of the four species increased with their calculated cell volume (Fig. 18). *C. wailesii* had the highest velocities and ranged from 30.4 m day^{-1} to

65.9 m day^{-1}, *H. cuneformis* from 12.4 m d^{-1} to 20 m d^{-1}, *P. calcar-avis* from 1.41 m d^{-1} to 3.45 m d^{-1}, and *Skeletonema spp.* from 1.09 to 4.01 m d^{-1}. Unpaired T-tests of heat killed treatments to average control treatments for both *C. wailesii* (avg=45.7 ± 17.5 m d^{-1}, n=84) and *H. cuneformis* (avg=14.0 ± 4.06 m d^{-1}, n=166) showed a significant difference with a p value of <0.00001. This verifies that the treatments had a sub lethal effect, as maximum sinking velocities were not reached for these two species.

EFFECT OF CRUDE OIL ON MEAN SINKING SPEED

Particle tracking results in 40-50 separate measurements of individual cells that comprise the population. Unlike traditional bulk methods, a histogram of results is a representation of how sinking speeds vary within the sample. Histograms of all species over time (Fig. 19a-d) visually represent the population distribution shape by treatment. A typical dose yield response curve would shift the population distribution to the right. Means and error bars representing standard deviation are generated from this data to examine the effects of treatment and time. There is no consistent increase or decrease in mean sinking speeds relative to the control in *C. wailesii, P. calcar-avis,* and *Skeletonema spp.,* (Fig. 20) while in *H. cuneformis* all oil treatments exhibited an increased sinking speed except the one-week high oil treatment.

The treatment concetrations used for *C. waileseii* were 10% of the concentrations used in our other species. Histograms of *C. wailesii* (Fig. 19a) did not show a typical yield-dose response curve of population shift in most treatments. *C. wailesii* at the 1-hour time point (Fig. 20) showed no visual increase in mean sinking rate relative to the

control. At the 6-hour time point *C. wailesii* showed a slight increase in sinking rate relative to the control. At the 24-hour time point *C. wailesii* showed increased sinking in the low oil treatment, but a decrease in the high oil treatment. Chi-squared analysis was used to test if treatments were significantly different from the control, as visual representation was difficult to interpret. Chi-squared analysis (Table 3) notes significant differences from the control in all time points with a p-value of <0.05. While the distributions were significantly different than the controls, the change in means was unpredictable, with both increases and decreases with treatments.

Histograms of *P.calcar-avis* showed this unpredictable yield-dose response in the low oil treatment (Fig. 19b). *P.calcar-avis* showed a slightly decreased sinking speed (Fig. 20) in the 1-hour and 1-day oil treatments but an increase in the high oil treatment at all time points, with significant differences (p-value <0.05) in all treatments from chi-squared analysis (Table 3).

Histograms of *Skeletonema spp.* (Fig. 19c) did not show a typical yield-dose response over time in any treatment. None of the treatments (Fig. 20) showed a consistent increase in mean sinking speed. *Skeletonema spp.* showed no significant difference from the chi-squared analysis (Table 3) for the low oil treatment at the 1-hour mark (p-value=0.06), and also in the high oil treatment at the 1-hour (p-value=0.99) and 1-day time point (p-value=0.38). The 1-week time point noted significant differences in both oil treatments (p-value=0.002 low oil, p=0.00002 high oil), which were lower than the control.

Histograms of *H. cuneformis* (Fig. 19d) and mean sinking speeds of treatment (Fig. 20) do show an increase in sinking speed in all oil treatments except the 1-week high oil. *H. cuneformis* had significant chi-squared differences (Table 3) except in the 1-week low oil treatment (p-value=0.14).

EFFECT OF DISPERSANT ON MEAN SINKING SPEED

The low dispersant treatment in *C. wailesii* resulted in no increase in sinking speed at the 1-hour time point, but resulted in increases in sinking speed at 6-hours and 24-hours (Fig. 20). High dispersant treatments showed increased sinking rate at all time points for *C. wailesii.* All dispersant treatments were significantly different from the control (Table 3) with a p-value of <0.05.

P. calcar-avis showed increased sinking relative to the control in all dispersant treatments at all time points except the 1-week high dispersant treatment. All dispersant treatments were significantly different from the control (Table 3) with a p-value of <0.05.

Skeletonema spp. had similar or decreased sinking speeds in all dispersant treatments except the initial high dispersant treatment (Fig. 20) although the abnormally high values suggest error. All dispersant treatments were significantly different from the control (Table 3) with a p-value of <0.05.

H. cuneformis shows an increase in sinking rate (Fig. 20) with all dispersant treatments except the 1-week low dispersant treatment. Chi-squared analysis shows significant differences in all dispersant treatments except the 1-week low dispersant in *H.*

cuneformis. The initial high dispersant exposure treatment in all species caused a large increase in mean sinking rate (Fig. 20).

EFFECT OF CRUDE OIL AND DISPERSANT MIXTURE ON MEAN SINKING SPEED

Addition of crude oil and chemical dispersant in most treatments did not result in a consistent yield dose response of mean sinking rate relative to the controls with respect to concentration (Fig. 20). Chi squared analysis shows significant differences from the control in all treatments except the 1-day low mixture treatment with a p-value of <0.05. The highest recorded sinking values for each species except *Skeletonema spp.* was in one of the high mixture treatment time points. In *C. wailesii,* the 6-hour and 24-hour time point mixture treatments both showed increases relative to the control. *P. calcar-avis* showed increased sinking speeds for both mixture treatments at the 1-week time point. *Skeletonema spp.* had decreased sinking speeds for both mixture treatments at all time points except the 1-hour low mixture treatment. *H. cuneformis* showed increased sinking speeds for both mixture treatments at all time points.

EFFECT OF TIME ON MEAN SINKING SPEED

The time series (Fig. 21) of *C. wailesii* shows an increase in the low oil treatment and low mixture treatment, and decreases in the high dispersant treatment. Other treatments exhibited stagnant, increased, and/or decreased sinking over time. In *P. calcar-avis,* there was no clear trend over time except the high mixture treatment (Fig.

21). *Skeletonema spp.* showed an increase in the low oil treatment and high mixture treatments, with a decrease over time in the low mixture treatment (Fig. 21). *H. cuneformis* (Fig. 21) showed a decrease in the high oil treatment and high mixture treatment. A consistent trend among species is that the low oil treatment tended to increase sinking speed over time, while the higher oil treatment tended to decrease sinking.

POPULATION DISTRIBUTION BY SKEWNESS VERSUS KURTOSIS

Population distribution characteristics are compared to the expected distribution of the control by use of the chi-square value. Significant differences indicate changes in the distribution although the means may not show apparent differences. The skewness and kurtosis values assist in visualizing any changes in central tendency or kurtosis. The calculated values themselves show no clear trend (Table 4) within treatment levels. A skewness kurtosis bi-plot is an easier way to visualize the data matrix (Fig. 22). *Skeletonema spp.* tends to have higher skewness values, representing a left skew, while *H. cuneformis* tends to stay normally distributed or skewed to the right. *H. cuneformis* also showed a trend in kurtosis values, where the weekly treatments showed the tendency to form larger peaks in their distribution.

Discussion

The goals of this study were to (1) determine whether crude oil elicits a change in the sinking response in marine diatoms and (2) whether these effects change over time, with higher concentrations, and with the addition of chemical dispersant. This allows a generalized understanding of how diatom sinking is affected in the presence of crude oil and chemical dispersant. This study utilized crude oil concentrations known to be sub-lethal to a variety of marine phytoplankton (Ozhan & Bargu 2014b, Ozhan et al. 2014b). The sinking rates in experiemental treatments were less than the dead cell sinking rates, indicating that the oil exposure did not kill the cells. With the water-accommodated fraction technique, physical effects of large oil droplets such as adhesion to the frustule can be negated and thus only physiological effects on sinking rates were observed.

Similar to Harrison et al.'s observations (1986), there was no clear increase in sinking rate with oil and dispersant exposure in most treatments. However, Harrison et al. (1986) recorded a enclosed population with many changing variables over time such as nutrient concentration, nitrogen transport rates, chlorophyll *a*, and abundance over time, while our experiment was a controlled study on just the effects of crude oil and dispersant. While there were increases in sinking rate in some experimental conditions, the overall pattern was not indicative of an oil-effect on sinking rates. The calculated mean sinking rates from each population showed no consistent trend with treatment, concentration, or time except *H. cuneformis*. *H. cuneformis* exhibited an increased sinking rate in all treatments at all time points (Fig. 21) except the 1-week low dispersant

treatment. This was the only species to show a yield-dose response with respect to each time point. The variation in sinking ranges from all treatments implies that any effects are subtle and less than the variation induced by the measurement technique. There were significant differences in most distributions relative to the control according to the chi-squared analysis, but no consistent changes with respect to any treatment. While not predictable, the highest sinking speeds were found in one of the time points of the highest treatment mixture of crude oil and dispersant. It is hard to define if these effects were significant as no typical yield-dose response was shown except in *H. cuneformis*. This method of video filming may not have allowed clear resolution of the population sinking rate, which is discussed below.

The time series (Fig. 21) of each treatment shows there is no well-defined correlation within treatment type. Kurtosis and skewness were calculated to find other trends in population distribution besides mean sinking rate. Changes in central tendency and kurtosis did not bring to light any potential shifts in population distribution, although there are likely species-specific responses to these treatments. This is apparent in the bi-plot of skewness and kurtosis (Fig. 22) that shows *H. cuneformis* populations are generally situated on the higher end of the skewness scale, so the population is shifted to the left. Another trend in skewness is observed for *Skeletonema spp.* where populations are generally located on the lower end of the scale and thus shifted to the right. We would expect species that are increasing sinking rate in response to the treatments would respond by shifting the histogram to the right, therefore *Skeletonema spp.* is possibly

showing the most sensitivity to our treatments although effects are still difficult to quantify.

Diatoms are likely physiologically taxed from the experimental treatments, as similar concentrations have shown detrimental effects to marine diatoms (Pulich et al. 1974, Harrison et al. 1986, Parson et al. 1976, Lee et al. 1977, Hsiao et al. 1987). Also, less cell growth and increased mucilage was observed with the oil and oil & dispersant treatments, although these parameters were not quantified in this experiment. However, in this case, crude oil and chemical dispersant do not consistently elicit an increased sinking response. There has been one other chemical physiological stressor study on diatom sinking rate; Smayda (1974) found increased sinking rates in two freshwater diatoms *Asterionella formosa* and *Tabellaria flocculosa* with treatment of isopropanol and butanol. It is difficult to extrapolate results from this work and ours because Smayda (1974) used settling columns, which have been shown to have differences from the video-filming method (O' Brien et al. 2006). However, it shows that phytoplankton sinking is affected by physiological stress, in which case it would have been helpful to assess the physiological state of the cells in our experimental treatments.

There are also other factors that must be considered for analysis in this work, for example the nature of this filming method only captures a fraction of the population, and thus may not be a full representation of the sinking distribution. Also, while sinking rates are thought to be constant in marine phytoplankton which may not be the case. Recent observations indicate that *C. wailesii* and *H. cuneformis* instantaneously modifying their sinking acceleration rates (Gemmell et al. in prep). The lack of a typical dose-response

curve in these treatments is puzzling. Even with the these potential sources of variation; if the mean sinking rate of the population shifted right, the effect should be amplified by our filming methodology, as these cells would appear first in our viewing window.

Diatom sinking is an important characteristic to better understand their population success and distribution within the water column, as well as an important metric of information for oceanic carbon budgets. This was the first laboratory controlled study to quantify how diatom sinking is affected by crude oil and chemical dispersant. The next step would be to assess the full sinking distribution tendencies within natural populations and to find a concentration of oil that will definitively elicit a sinking response in diatoms. This study observed a pattern of no tangible effect of crude oil and chemical dispersant on diatom sinking rates and suggests that, single cell diatom loss through sinking will not be enhanced by exposure to crude oil and chemical dispersant. The lack of a sinking response warrants further studies into how they are physiologically affected by crude oil, along with studies on the biophysical model of phytoplankton suspension as suggested by Smayda (1974).

This new method of observing particle sinking studies shows promise in a variety of studies, although more work is needed to fully verify its accuracy in capturing the full range of sinking distributions for phytoplankton. The major caveats in using this technique for sinking studies are that it does not capture the full population and likely misses many slower sinking cells. When compared to SETCOL rates, the video filming method records higher sinking speeds (O'Brien et al. 2006), strengthening the idea that this technique is limited in capturing the slowest sinking cells within a population. A

deeper comparison to the SETCOL technique and the laser-scanning method would help verify its accuracy. A limitation in the recording time is that increasing video length exponentially increases compete processing time. One way to overcome this hurdle is by fully filming control populations and comparing it to shortened videos to establish how much distributions differ. If this technique can successfully be implemented for phytoplankton it will help quantify the differences in sinking within a population that can assess its vertical distribution within the water column.

Tables

State	**m/day**
Living	0-30
Palmelloid stages	~10-6150
Dead, intact	<1-510
Fragments	1.5-26 x 10^3

Table 1: A comparison of phytoplankton sinking rates in various conditions. Palmelloid is a stage where cells are attached to a mucilage matrix. Shows there are variable sinking rates within a population dependent on physiological state. From Smayda (1970).

Species	Crude oil	Response (EC_{50}, in milligrams per liter)	Duration	Reference
Monochrysis lutheri	Amoco Cadiz	4.4	2 hours	Vandermeulen et al. 1979
M. lutheri	Bunker C	3.3	2 hours	Vandermeulen et al. 1979
Phaeodactylum tricornutum	Arabian light	16.4	14 days	Siron et al. 1991
Dunaliella tertiolecta	Arabian light	36	14 days	Siron et al. 1991
Thalassionema frauenfeldii	Nigerian	>50	24 hours	Adekunle et al. 2010
Coscinodiscus centralis	Nigerian	>50	24 hours	Adekunle et al. 2010
Ceratium trichoceros	Nigerian	>50	24 hours	Adekunle et al. 2010
Odontella mobiliensis	Nigerian	>50	24 hours	Adekunle et al. 2010
Chaetoceros socialis	South Louisiana	1.84	10 days	Ozhan et al. 2014
Ditylum brightwellii	South Louisiana	2.50	10 days	Ozhan et al. 2014
Heterocapsa triquetra	South Louisiana	1.03	10 days	Ozhan et al. 2014
Pyrocystis lunula	South Louisiana	1.75	10 days	Ozhan et al. 2014
Scrippsiella trochoidea	South Louisiana	1.14	10 days	Ozhan et al. 2014

Abbreviation: EC_{50}, half maximal effective concentration.

Table 2: Historical cell death responses of phytoplankton to crude oil in previous studies. Shows historic dosage as EC50, which represents growth inhibition. For *Ditylum brightwelli,* a concentration of 2.50 mg L^{-1} resulted in EC50 in growth inhibition. From Ozhan et al. (2014a).

		C-Test p-value	Sig. Chi-Squared?	Skewness	Kurtosis
Coscinodiscus 1 Hour	CONTROL			-0.45	-1.44
	WAF L	$5.85x10^{-14}$	Y	1.10	0.62
	WAF H	$6.78x10^{-7}$	Y	0.51	0.43
	DISP L	$2.88x10^{-10}$	Y	0.06	-0.98
	DISP H	$4.43x10^{-5}$	Y	-0.04	-0.64
	CEWAF L	$6.96x10^{-4}$	Y	-0.55	-0.59
	CEWAF H	$3.61x10^{-2}$	Y	0.37	-0.22
6 Hour	CONTROL			0.21	-1.11
	WAF L	$3.60x10^{-6}$	Y	-0.58	-0.18
	WAF H	$1.92x10^{-3}$	Y	-0.24	-0.77
	DISP L	$1.96x10^{-10}$	Y	0.01	-0.94
	DISP H	$1.25x10^{-7}$	Y	-0.22	-1.05
	CEWAF L	$1.14x10^{-2}$	Y	-0.73	-0.71
	CEWAF H	$9.73x10^{-5}$	Y	-0.05	-0.80
24 Hour	CONTROL			0.07	-0.95
	WAF L	$7.86x10^{-10}$	Y	0.74	0.20
	WAF H	$4.75x10^{-3}$	Y	0.17	-1.58
	DISP L	$8.65x10^{-23}$	Y	0.16	0.57
	DISP H	$9.17x10^{-17}$	Y	-0.94	1.99
	CEWAF L	$1.55x10^{-15}$	Y	0.57	-0.88
	CEWAF H	$3.62x10^{-2}$	Y	0.28	-1.04

a. *Coscinodiscus wailesii*

		C-Test p-value	Sig. Chi-Squared?	Skewness	Kurtosis
Pseudosolenia 1 Hour	CONTROL			0.89	-0.35
	WAF L	$3.81x10^{-6}$	Y	0.91	0.15
	WAF H	$2.44x10^{-13}$	Y	2.33	8.46
	DISP L	$1.93x10^{-27}$	Y	-0.37	0.26
	DISP H	$7.20x10^{-48}$	Y	-0.47	-0.81
	CEWAF L	$1.29x10^{-2}$	Y	-0.42	-0.87
	CEWAF H	$2.50x10^{-16}$	Y	0.95	0.95
1 Day	CONTROL			0.94	0.81
	WAF L	$8.48x10^{-27}$	Y	-0.40	0.64
	WAF H	$3.70x10^{-5}$	Y	0.52	0.16
	DISP L	$1.80x10^{-4}$	Y	-0.37	-0.38
	DISP H	$6.96x10^{-5}$	Y	0.53	-0.61
	CEWAF L	$3.48x10^{-10}$	Y		
	CEWAF H	$3.18x10^{-15}$	Y	0.03	-0.79
1 Week	CONTROL			0.47	-0.61
	WAF L	$9.67x10^{-4}$	Y	0.84	0.19
	WAF H	$3.79x10^{-6}$	Y	0.09	-0.32
	DISP L	$2.34x10^{-5}$	Y	0.04	-0.18
	DISP H	$1.76x10^{-2}$	Y	0.84	-0.27
	CEWAF L	$1.54x10^{-5}$	Y	0.96	2.39
	CEWAF H	$1.04x10^{-13}$	Y	0.84	0.13

b.*Pseudosolenia calcar-avis*

		C-Test p-value	Sig. Chi-Squared?	Skewness	Kurtosis
Skeletonema 1 Hour	CONTROL			1.59	2.80
	WAF L	5.89×10^{-2}	N	0.29	0.05
	WAF H	0.99	N	0.17	0.12
	DISP L	1.26×10^{-2}	Y	0.76	0.42
	DISP H	2.19×10^{-103}	Y	0.04	-0.68
	CEWAF L	1.86×10^{-4}	Y	0.03	-0.96
	CEWAF H	1.60×10^{-7}	Y	0.43	-0.74
1 Day	CONTROL			0.33	-0.41
	WAF L	1.93×10^{-3}	N	0.65	-0.46
	WAF H	0.38	Y	0.50	-0.57
	DISP L	3.25×10^{-6}	Y	1.03	0.72
	DISP H	6.69×10^{-4}	Y	0.74	1.01
	CEWAF L	1.67×10^{-4}	Y	0.78	0.12
	CEWAF H	6.43×10^{-5}	Y	0.31	-0.77
1 Week	CONTROL			0.51	0.20
	WAF L	1.65×10^{-3}	Y	0.58	-0.54
	WAF H	1.65×10^{-5}	Y	0.72	0.66
	DISP L	9.64×10^{-6}	Y	1.62	2.58
	DISP H	1.05×10^{-3}	Y	1.59	1.83
	CEWAF L	2.99×10^{-8}	Y	0.99	0.59
	CEWAF H	3.71×10^{-3}	Y	0.82	-0.69

c. *Skeletonema spp.*

		C-Test p-value	Sig. Chi-Squared?	Skewness	Kurtosis
Hemidiscus 1 Hour	CONTROL			-1.08	-0.19
	WAF L	1.72×10^{-9}	Y	-0.95	0.87
	WAF H	4.62×10^{-12}	Y	-0.11	-0.51
	DISP L	8.31×10^{-3}	Y	-0.15	0.07
	DISP H	2.62×10^{-14}	Y	0.14	-0.78
	CEWAF L	2.98×10^{-17}	Y	-0.42	0.22
	CEWAF H	1.18×10^{-14}	Y	-0.25	-0.23
1 Day	CONTROL			-0.16	-0.99
	WAF L	1.07×10^{-5}	Y	0.25	1.77
	WAF H	9.85×10^{-11}	Y	-0.67	0.93
	DISP L	2.23×10^{-5}	Y	0.08	0.33
	DISP H	3.4×10^{-4}	Y	0.04	-0.10
	CEWAF L	0.59	N	0.10	0.51
	CEWAF H	1.14×10^{-4}	Y	-0.36	-0.93
1 Week	CONTROL			-0.59	0.25
	WAF L	0.14	N	1.67	5.83
	WAF H	1.71×10^{-5}	Y	0.83	0.45
	DISP L	1.59×10^{-3}	N	-0.61	3.19
	DISP H	7.99×10^{-2}	Y	2.05	5.59
	CEWAF L	3.11×10^{-2}	Y	-0.35	2.74
	CEWAF H	2.73×10^{-2}	Y	0.35	1.27

d. *Hemidiscus cuneformis*

Table 3: Chi squared analysis of all treatments. Yes (Y) represents a 95% confidence interval that the treatment is significantly different from the control in terms of its distribution. The kurtosis and skewness were also analyzed to parse out any potential population direction, and are visually represented in Figure 22.

Figures

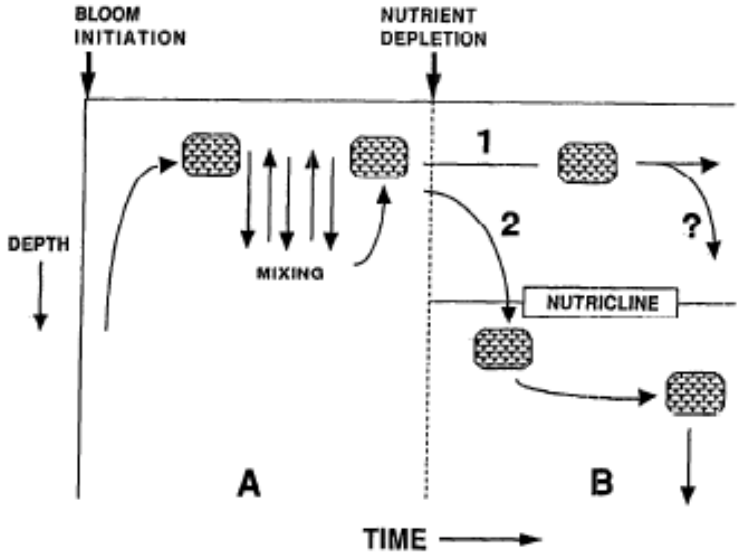

Figure 1: Conceptual model of diatom sinking control during a spring bloom. A. Light and nutrients are saturating, and cell sinking rates are limited by light availability. B. Limiting nutrients cause cells to either not respond (1) or leave the photic zone (2). Shows how biotic factors can control diatom distribution within a water column. From Waite et al. (1992).

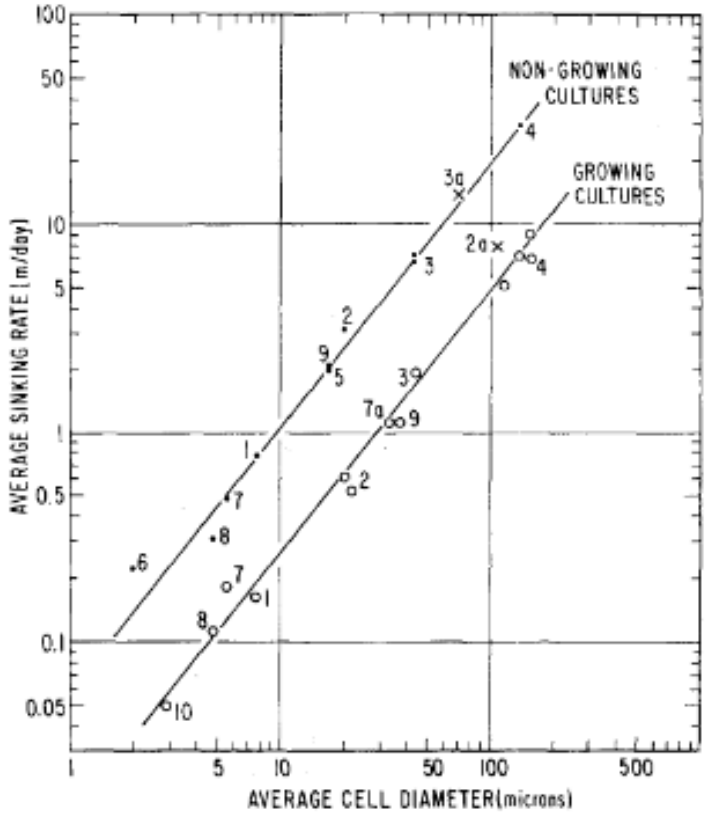

Figure 2: The relation of average sinking rate of unicellular diatoms from cultures and the average cell diameter. Sinking rate to cell diameter in unicellular diatom cultures. From Eppley et al. 1967, with included data from Gross & Zeuthen 1948, Smayda & Boleyn 1965, 1966.

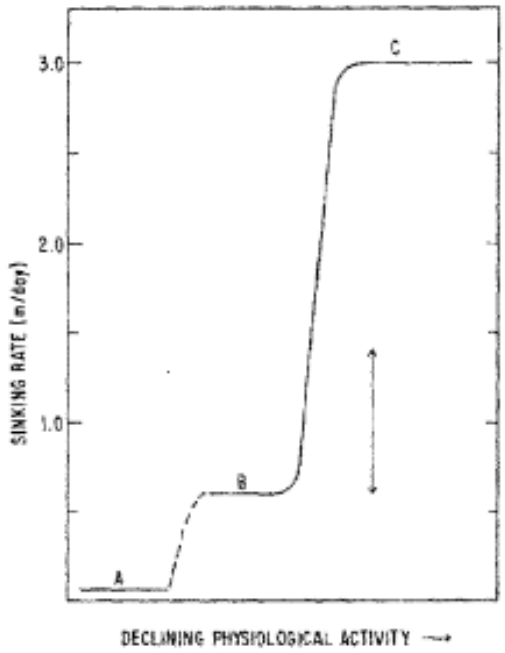

Figure 3: Sinking rates of *Ditylum brightwellii* in three hypothetical states. Differing physiological states: A. Neutrally-buoyant cells. B. Growing cells. C. Senescent cells. The vertical arrow indicates the range of sinking rates for growing cells. Sinking rates can vary greatly depending on the life stage. From Eppley et al. (1967).

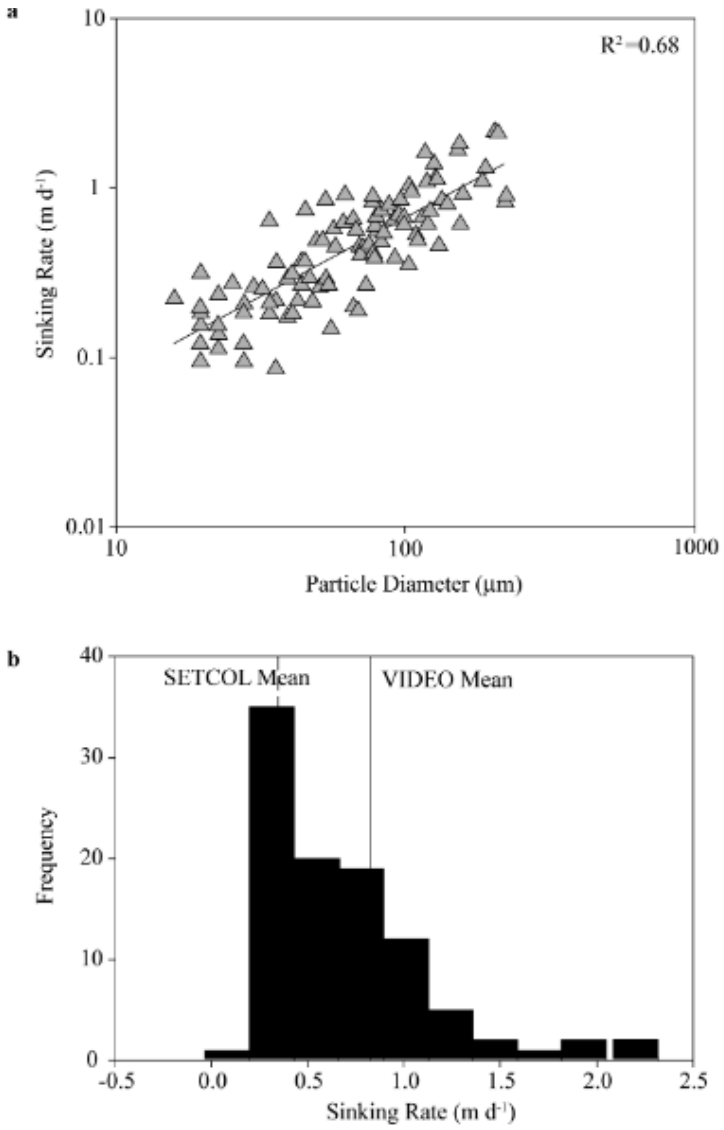

Figure 4: Sinking rates of *Skeletonema costatum*
(a) Size to sinking rate data of *Skeletonema costatum* from VIDEO.
(b) Histogram of sinking-rate measured using the VIDEO method.
Cells were present as a single cell or very short chains. In (b), the mean sinking rates indicated by SETCOL and VIDEO methods are noted and show differences in mean sinking rate between the two methods. From O'Brien et al. (2006).

Figure 5: Fate of marine oil spills. A schematic representing all the considered factors of how a marine oil spill interacts with the water column. There are many interactions that crude oil has with the water column. From McGenity et al. (2012).

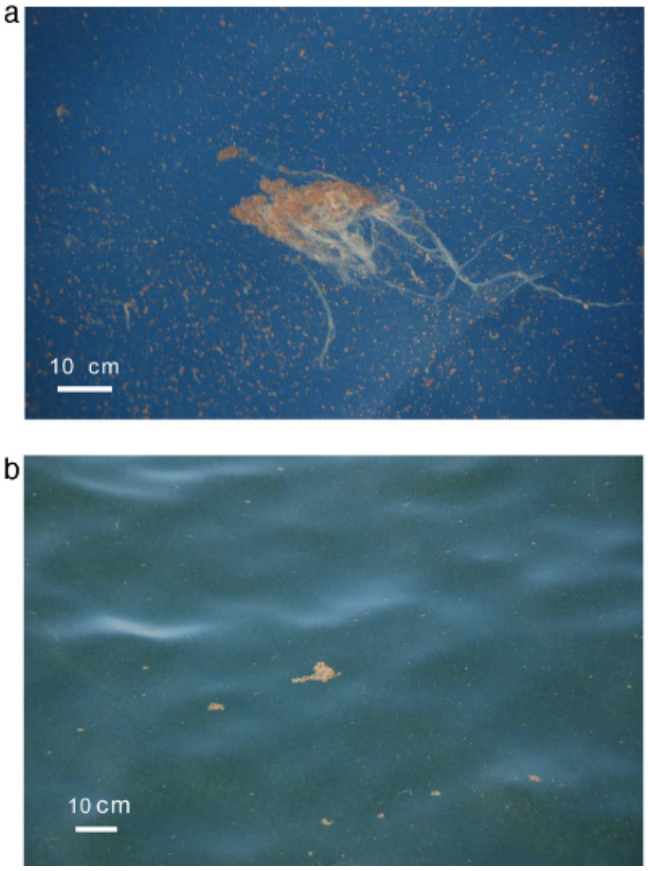

Figure 6: Mucous rich marine snow aggregates. Photographs of large, mucous rich marine snow particles in the surface shortly after the Deepwater Horizon spill. From Passow et al. (2012).

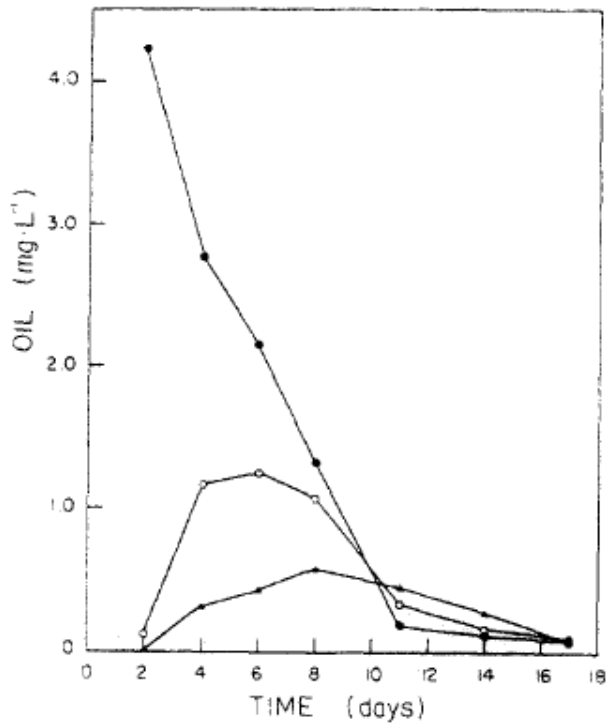

Figure 7: Changes in particulate oil concentration in CEE-3 (oil and dispersant). There were three depth intervals: 0-5 (Black dot), 5-10 (White dot) and 10-13 (Black triangle). Oil degrades overtime and can vary with depth. From Harrison et al. (1986).

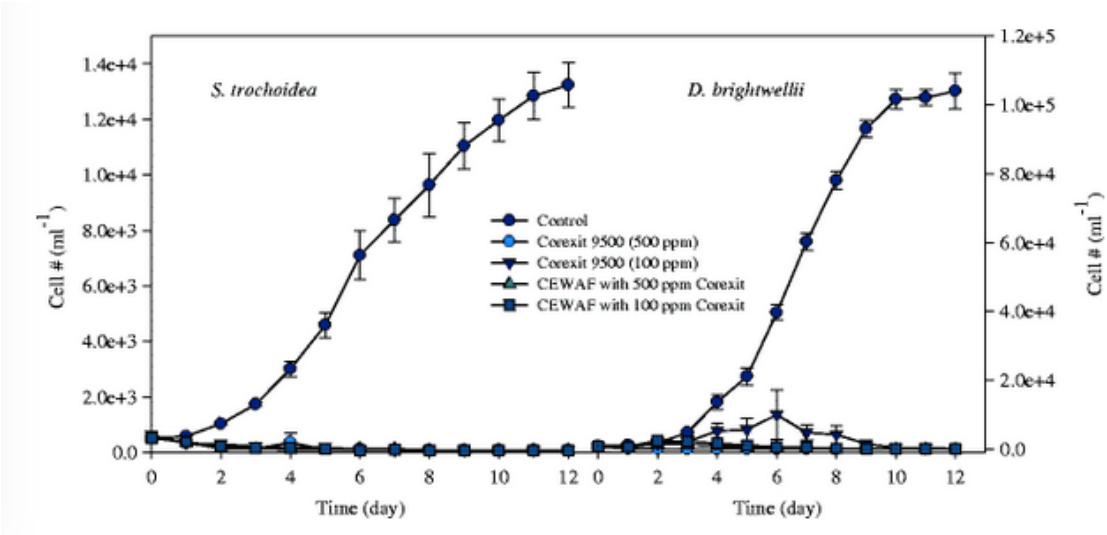

Figure 8: Diatom growth rate curve in Corexit and Corexit & LSC mixtures. Two species of diatoms and their abundance over a 12 day time period. Growth inhibition is observed from all experimental treatments for both species. From Ozhan et al. (2014b).

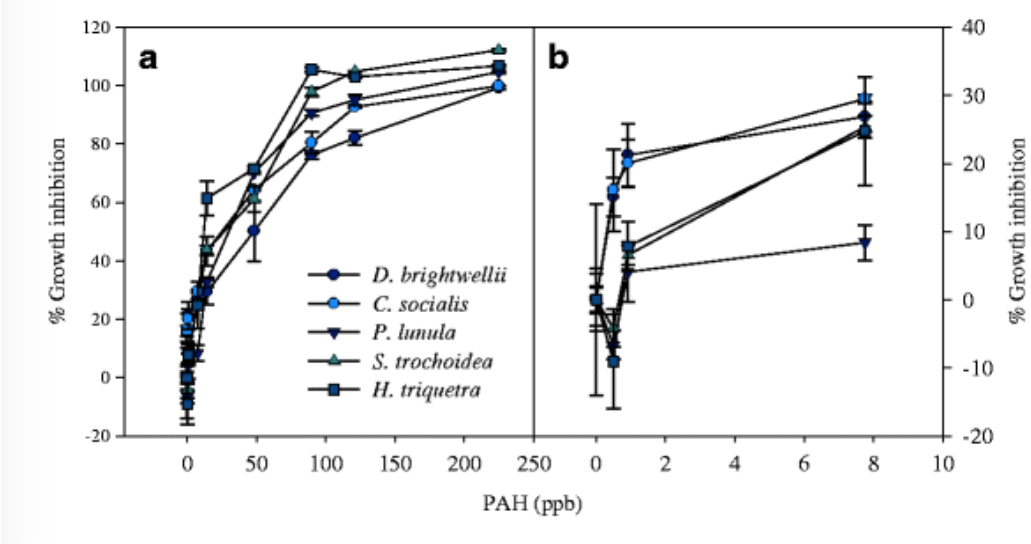

Figure 9: Growth rate inhibition of various diatom species with PAH. There is a correlation of increased growth rate inhibition with increased PAH concentration. From Ozhan et al. (2014b).

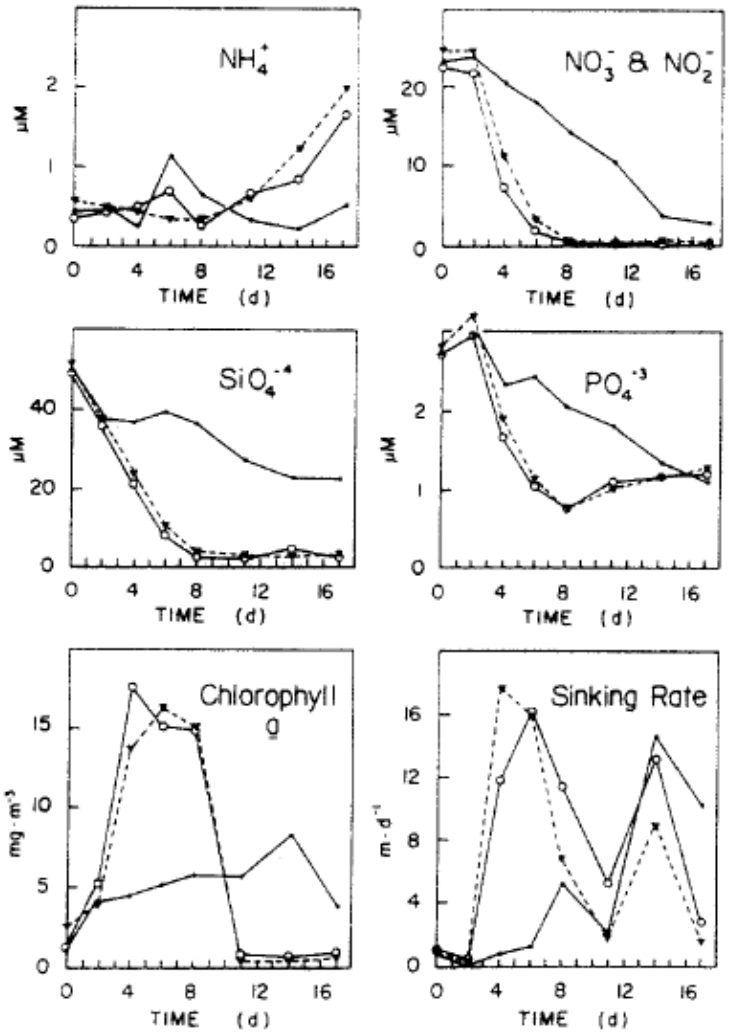

Figure 10: Changes in nutrients, chlorophyll *a*, and sinking rate of phytoplankton in experimental mesocosms. No observed sinking rate change with treatment; sinking rate spikes with nutrient levels around day 4. From Harrison et al. (1986).

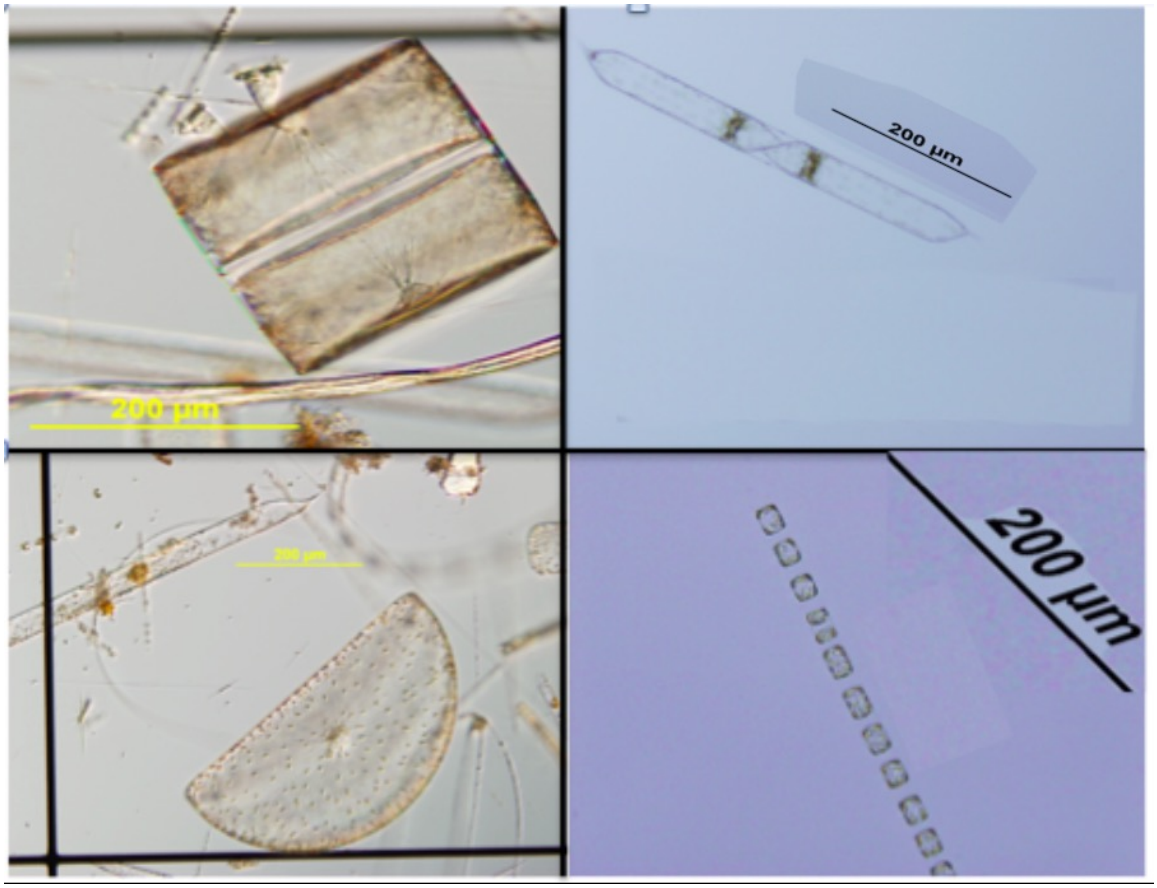

Figure 11: Species used in this study. Clockwise from the top left: *Coscinodiscus wailesii, Pseudosolenia calcar-avis, Skeletonema spp.,* and *Hemidiscus cuneiformis.*

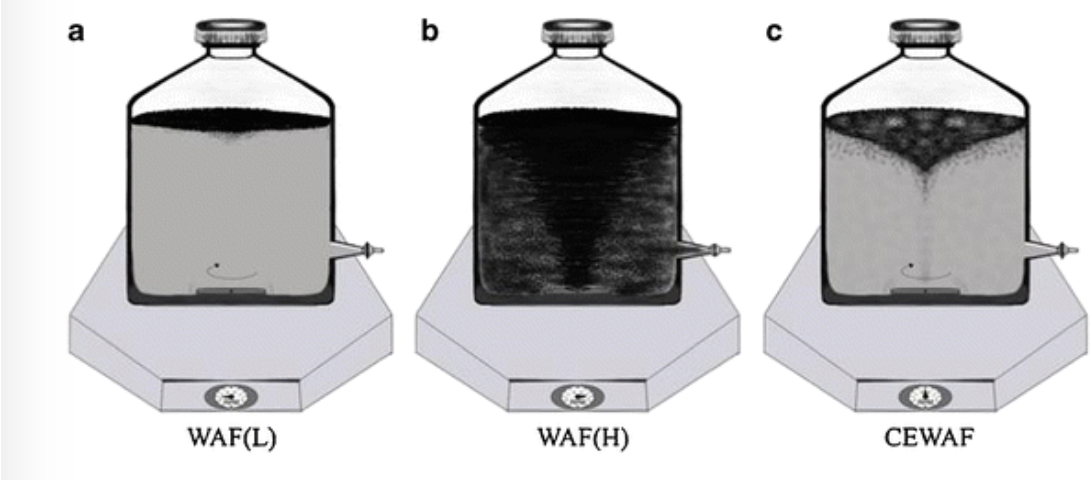

Figure 12: WAF and CEWAF preparation on low mixing shaker tables. A stir bar is used to slowly mix the oil and water for 24 hours, and then a 6 hour settling time is applied. The WAF and CEWAF is then extracted from the bottom valve to avoid disturbing the oil-water interface. From Ozhan et al. (2014b).

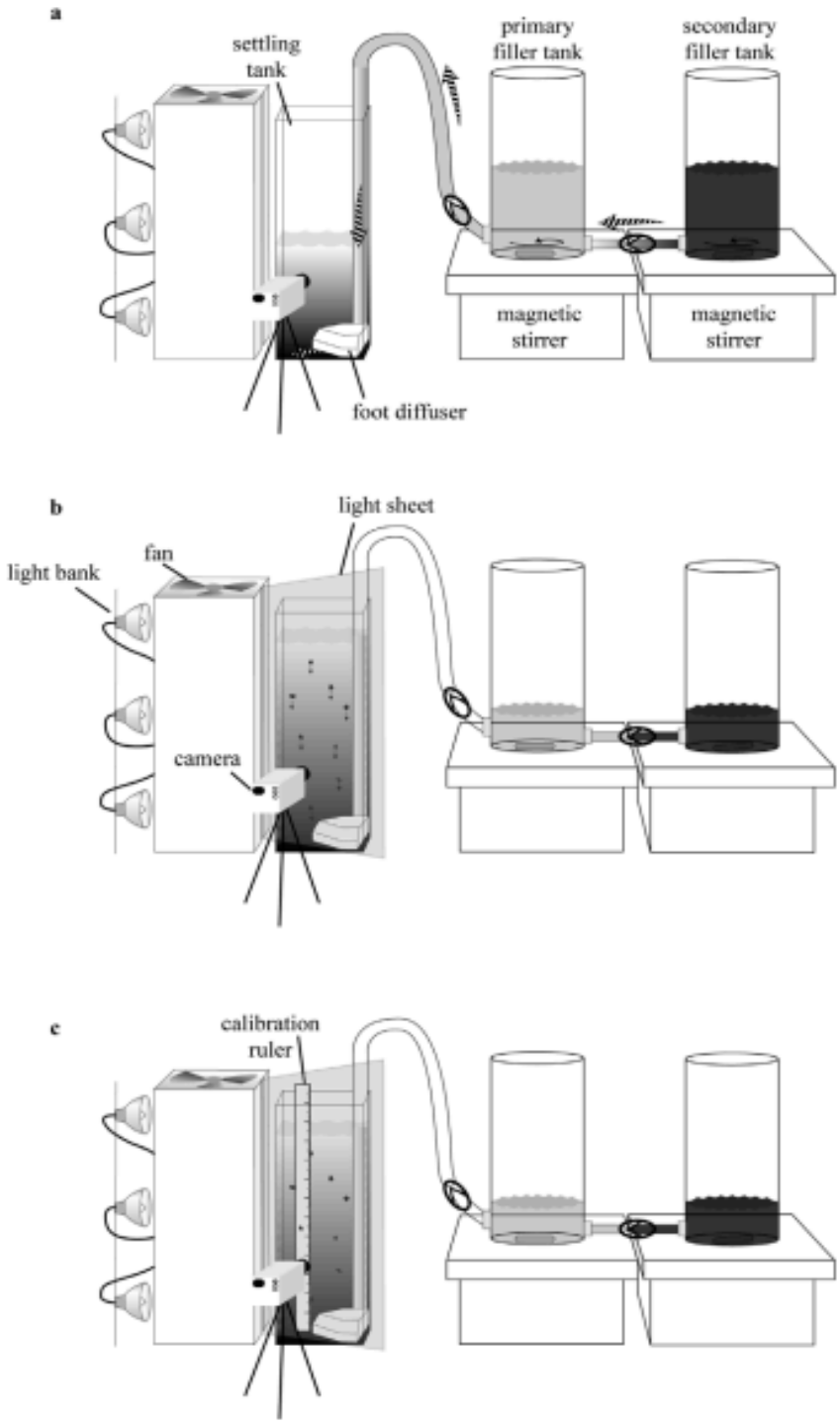

Figure 13: Imaging technique for phytoplankton sinking. Video records cells as they sink through a salinity gradient. Water is pumped from the primary filler tank (a) into the settling tank using a foot diffuser. Once the settling tank is filled (b), a light source is used to illuminate the column, and then particles are filmed (c) using a ruler for scale. From O'Brien et al (2006).

Figure 14: Diatom cells (*Coscinodiscus spp*.) sinking down a halocline. Color differences represent different salinities.

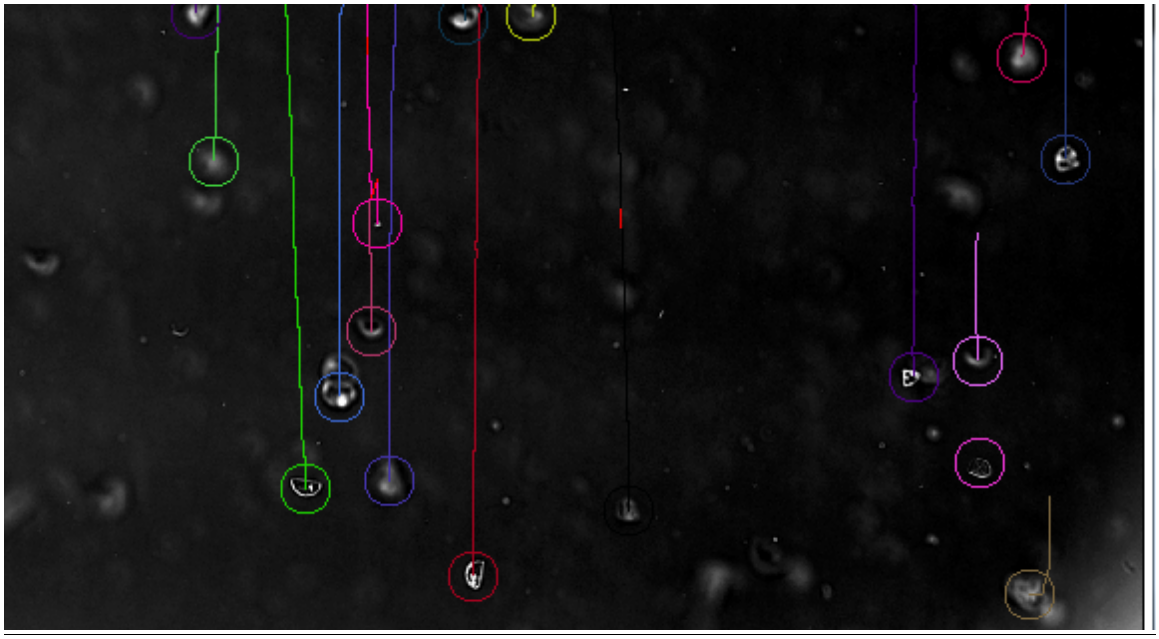

Figure 15: Individual particle trajectories. The lines represent the individual trajectories of *H. cuneformis* tracked by Image-J. In this case, the green, red, and purple trajectories were analyzed due to their crisper image, meaning they were more in focus to the depth of field.

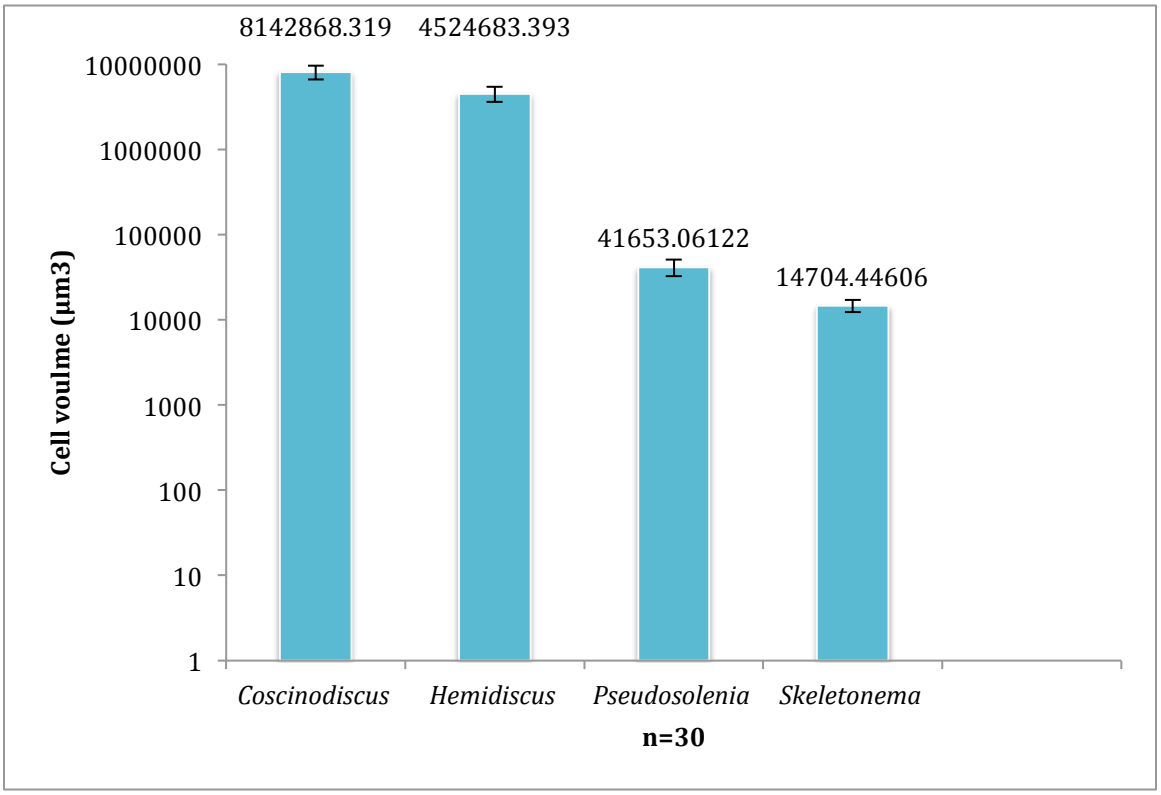

Figure 16: Cell volume calculations of the observed species. *C. wailseii* was by far the largest cell, followed by *H. cuneiformis*, and then *P. calcar-avis*, and *Skeletonema spp*. The average cell size (n=30) is listed above each species, and error bars represent standard deviations. Note the log scale on the y-axis.

a.

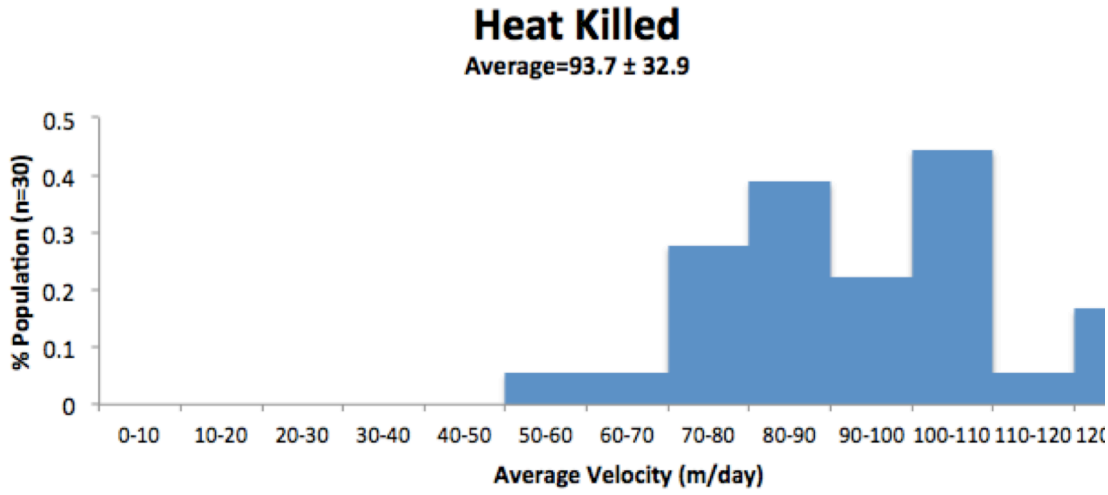

b.

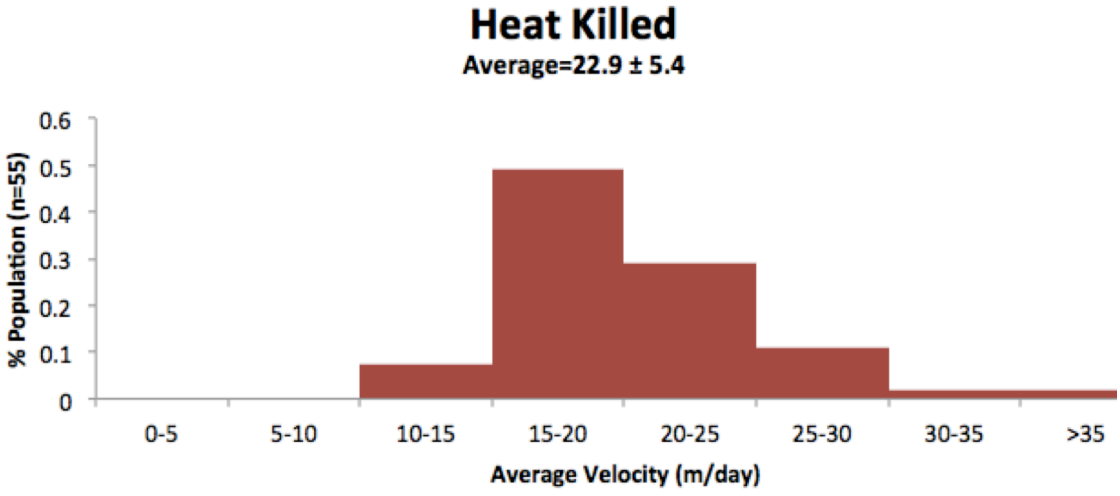

Figure 17: Heat-killed populations of *C. wailesii* (a) and *H. cuneformis* (b). Average sinking speeds are noted below the title. Population sizes are listed on the y-axis.

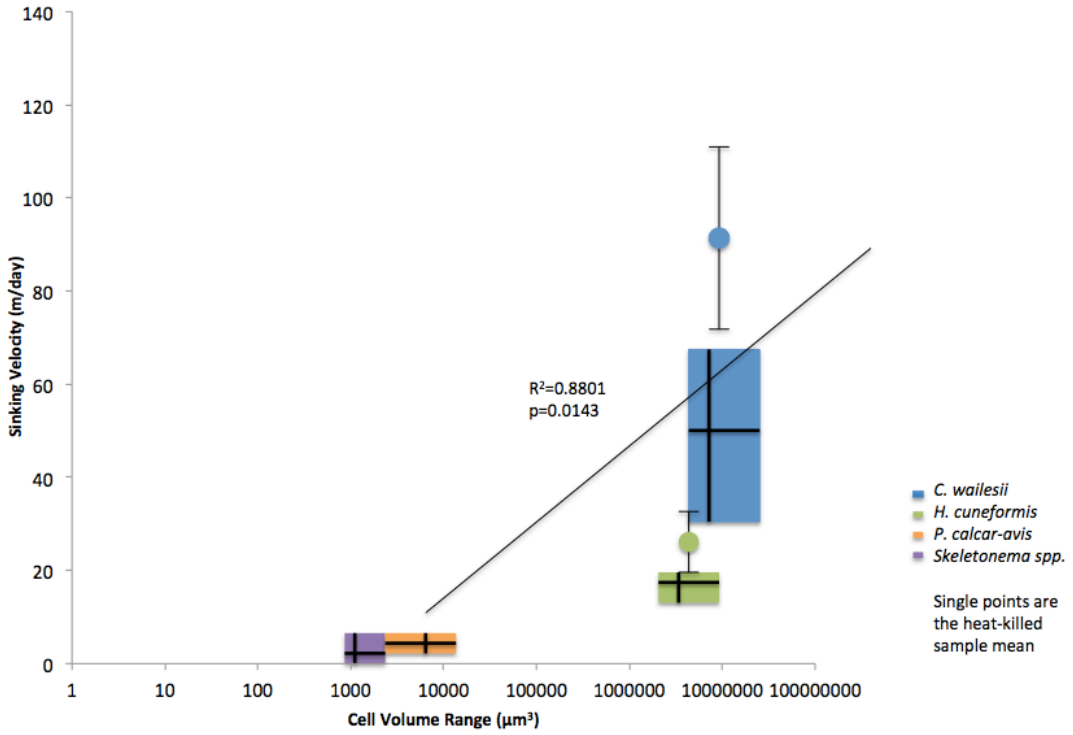

Figure 18: Cell volume range to average sinking velocities. The data presented is recorded from this experiment. Different colors represent different species, horizontal black lines are the average cell volume per species, and the vertical black lines are the average sinking volume per species. A linear regression was run using the sinking speeds and the average size of each species. The single points represent the heat-killed samples of the species, with error bars representing the standard deviation in these samples.

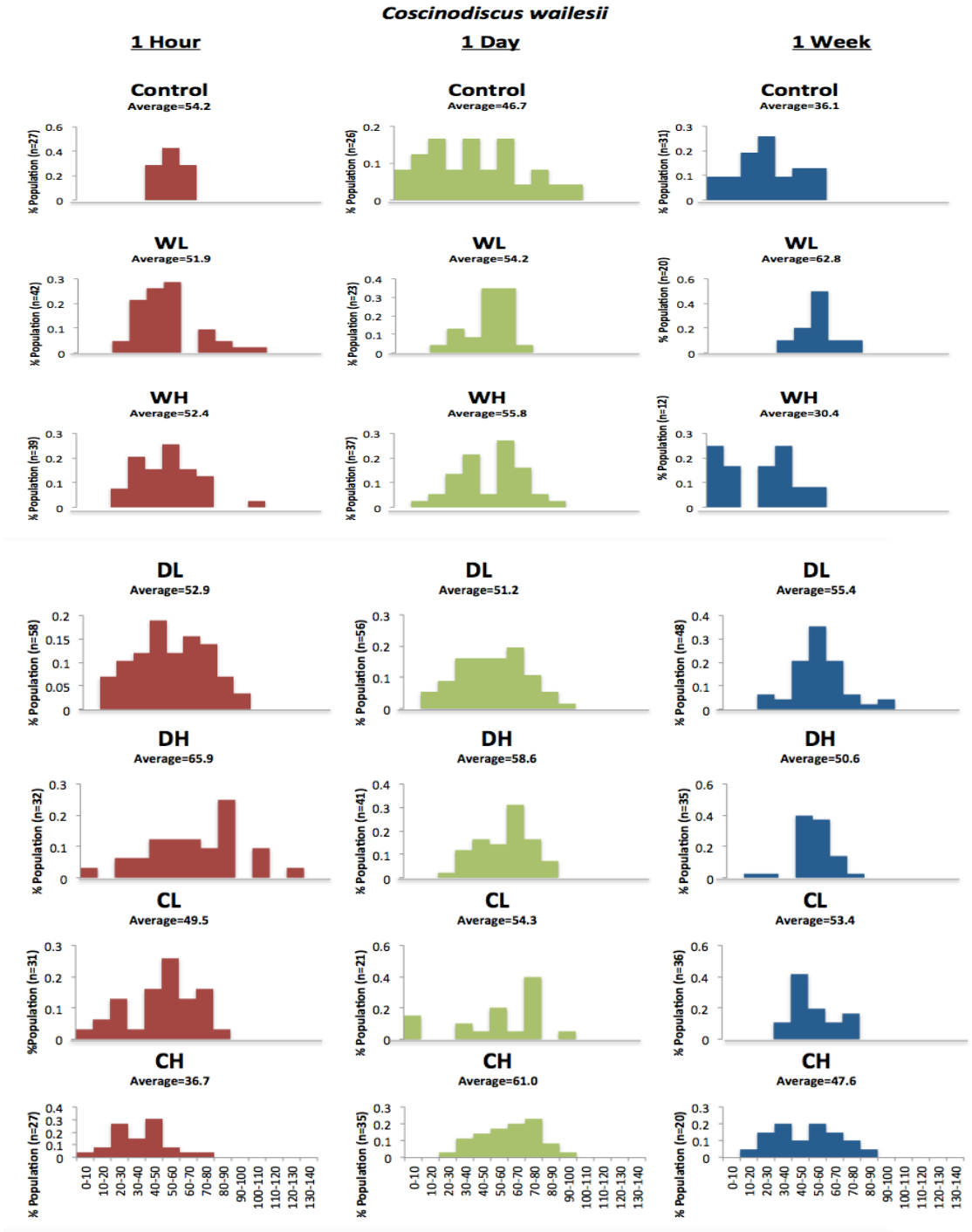

Figure 19: Treatment histograms by species.
a: Time series matrix for *C. wailesii*. From left to right represents increasing time period in each treatment. WL=Low WAF, WH=High WAF, DL=Low Dispersant, DH=High Dispersant, CL=Low CEWAF, CH=High CEWAF. Error bars are noted in Figure 20 and 21 on the individual bar plots.

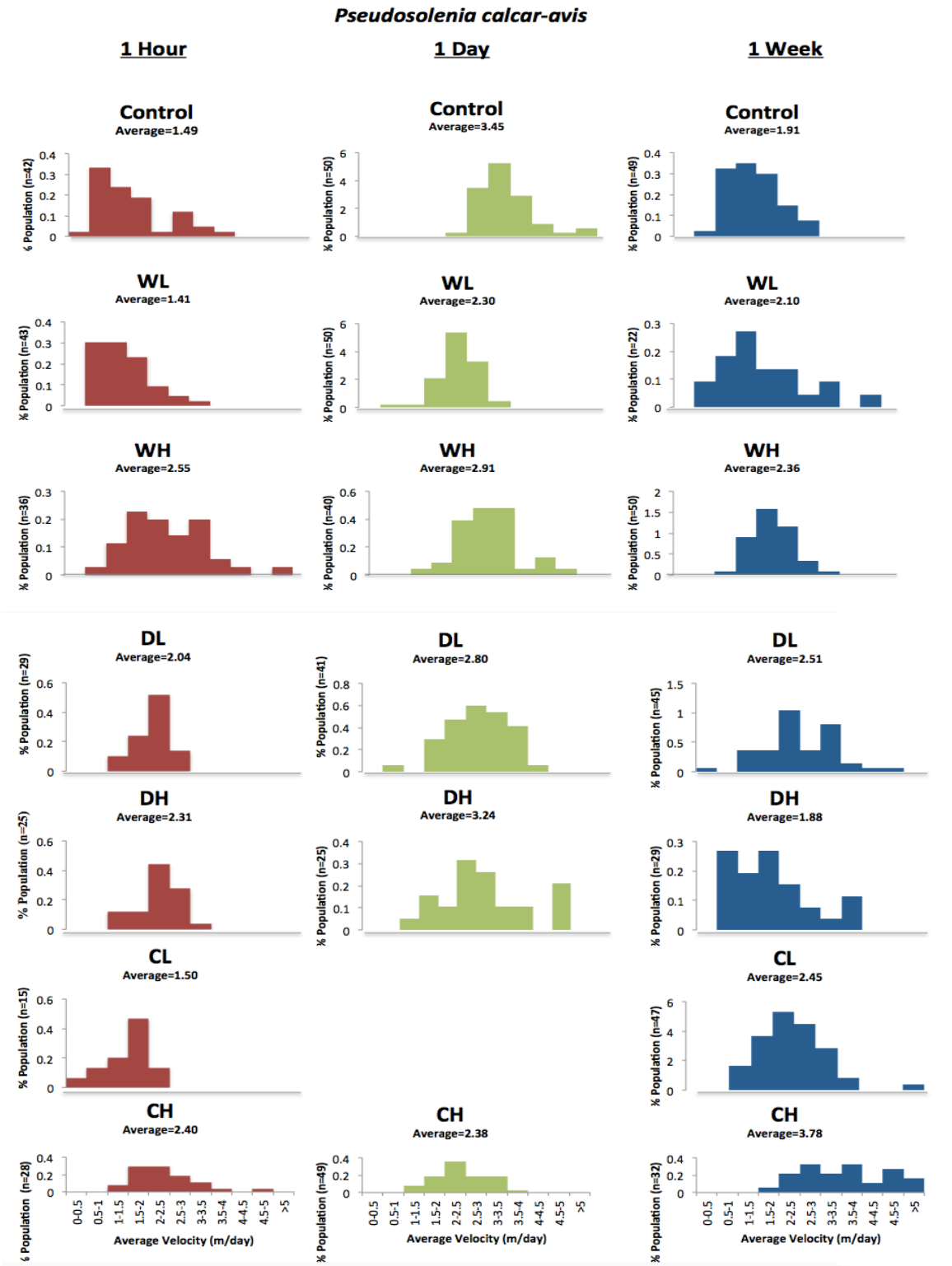

Figure 19b: Time series matrix for *P. calcar-avis*. There is one missing time point in *P. calcar-avis* due to file corruption.

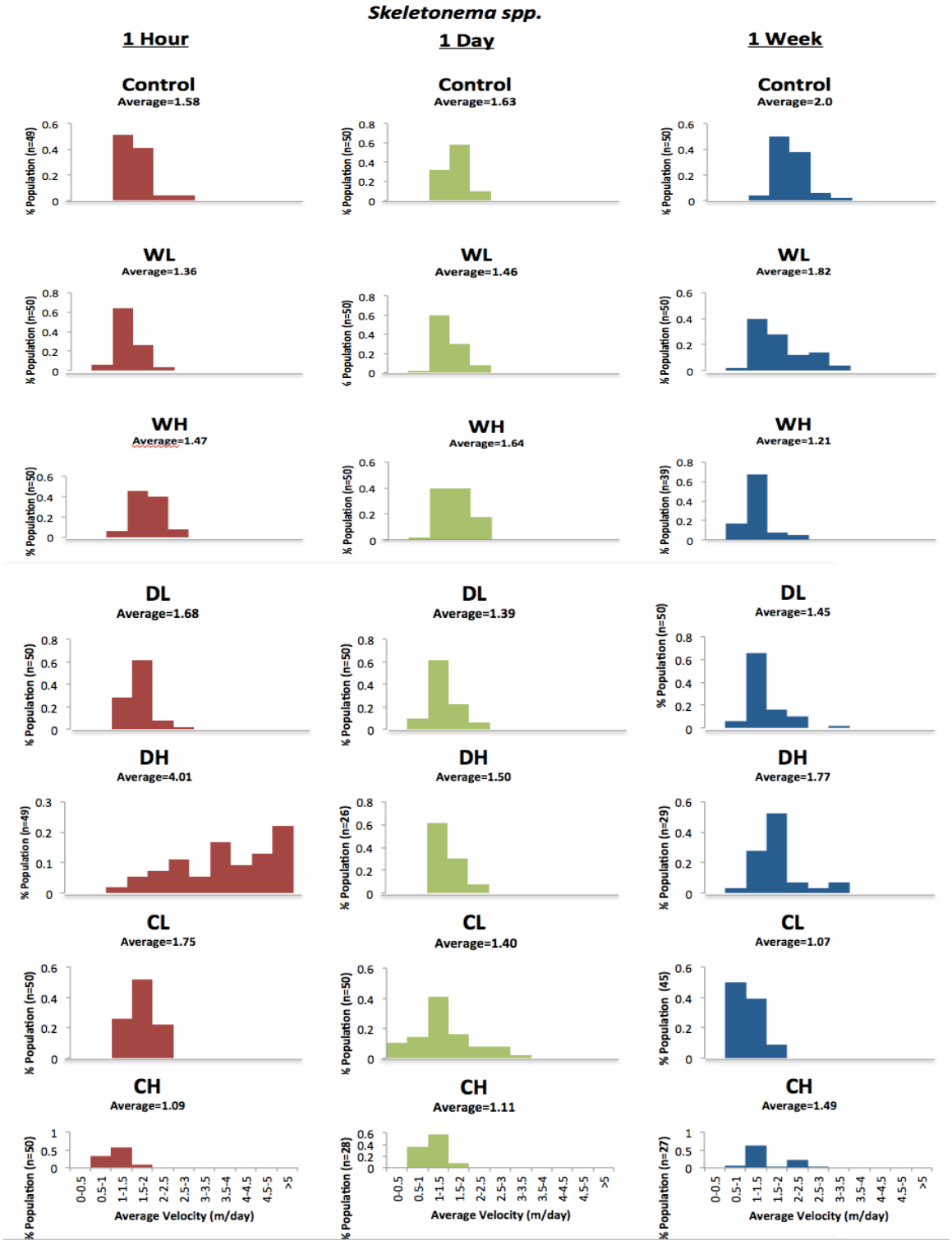

Figure 190c: Time series matrix for *Skeletonema spp.*

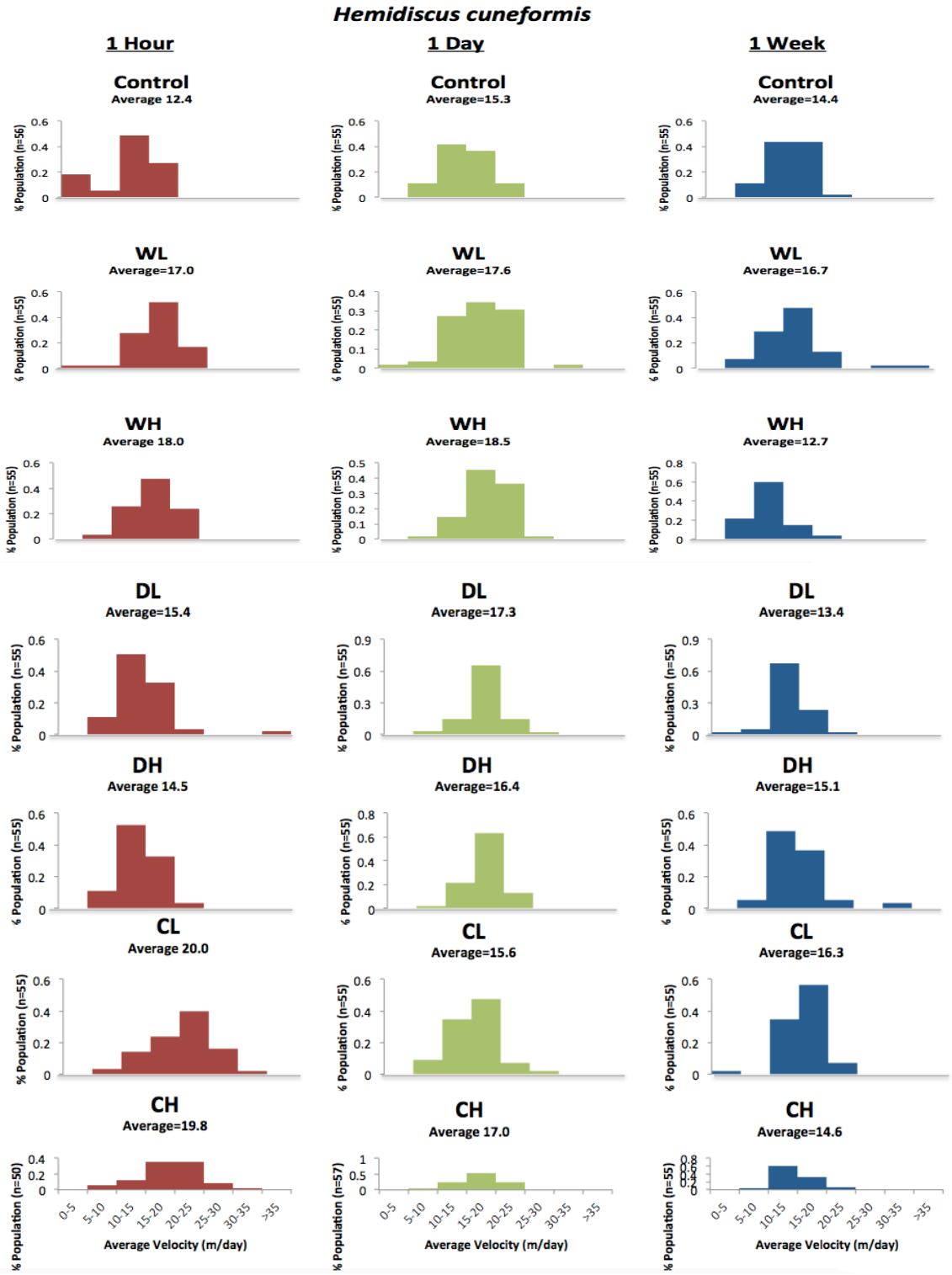

Figure 19d: Time series matrix for *H. cuneiformis.*

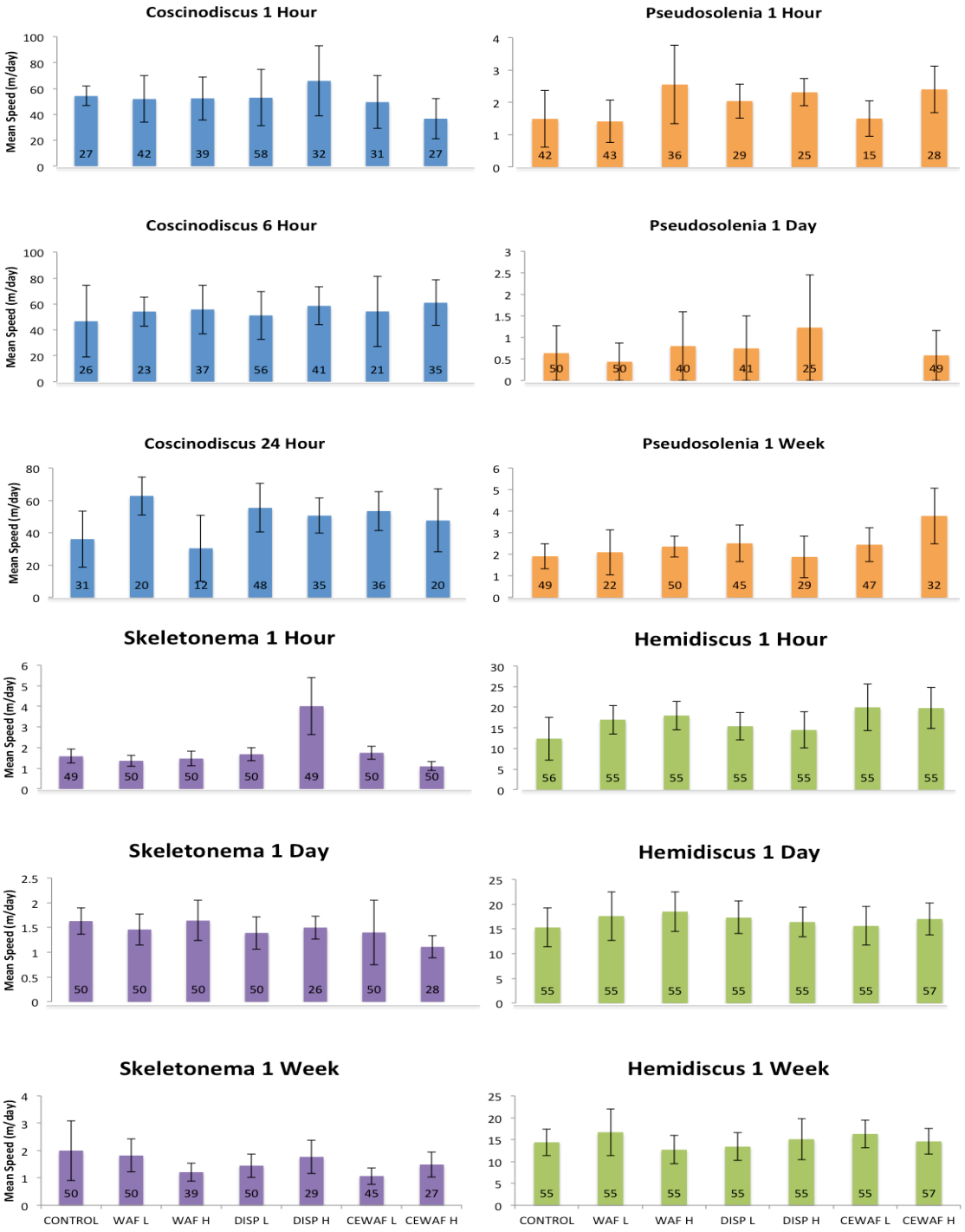

Figure 20: Mean sinking speeds of treatments per time point. Numbers at the base of each column is the n value per treatment. Error bars represent standard deviation.

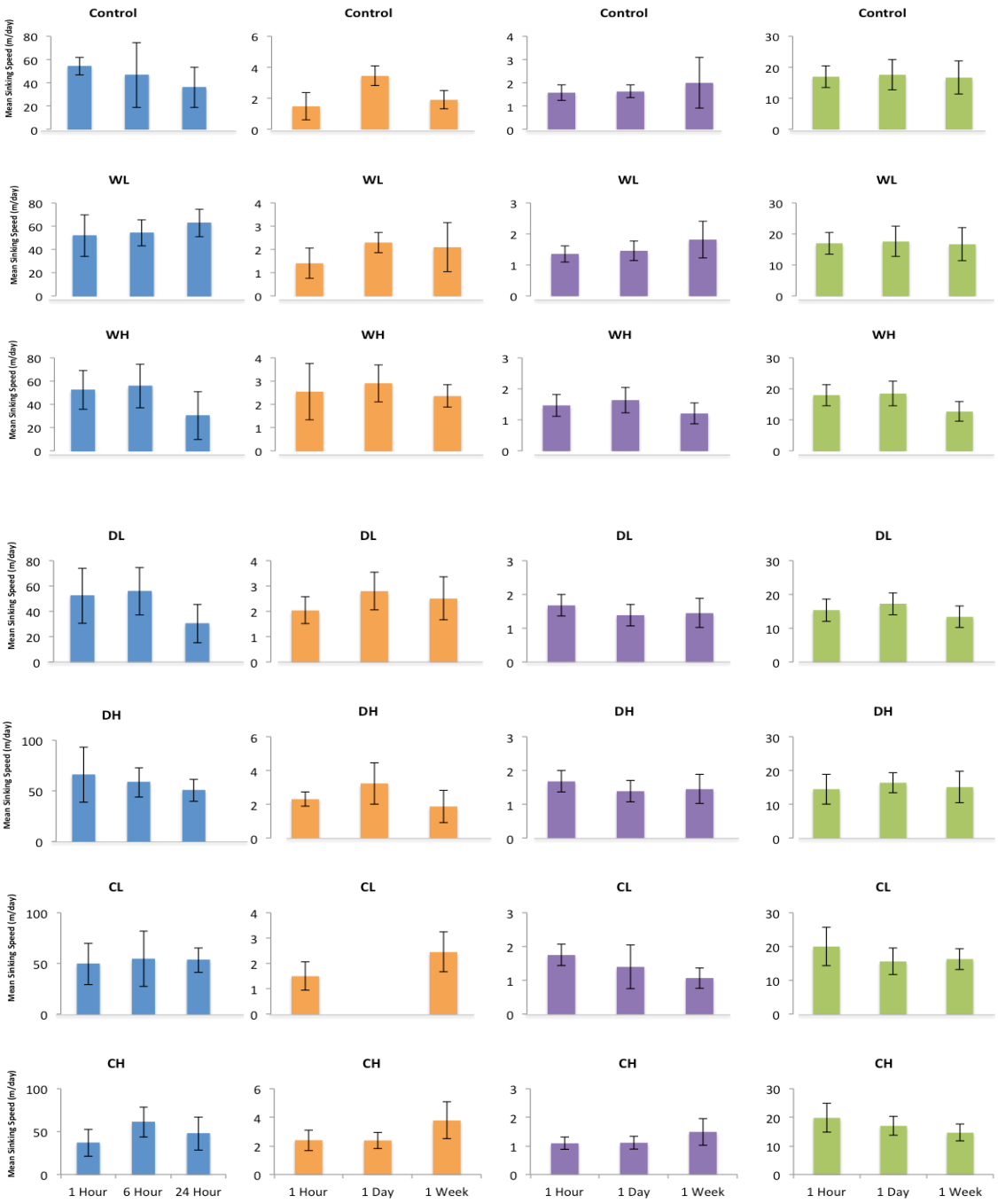

Figure 21: Mean sinking speeds of each treatment over time. Each color represents a different species: Blue=*C. wailesii,* Orange=*P. calcar-avis,* Purple=*Skeletonema spp.*, Green=*H. cuneformis.* Error bars represent standard deviation.

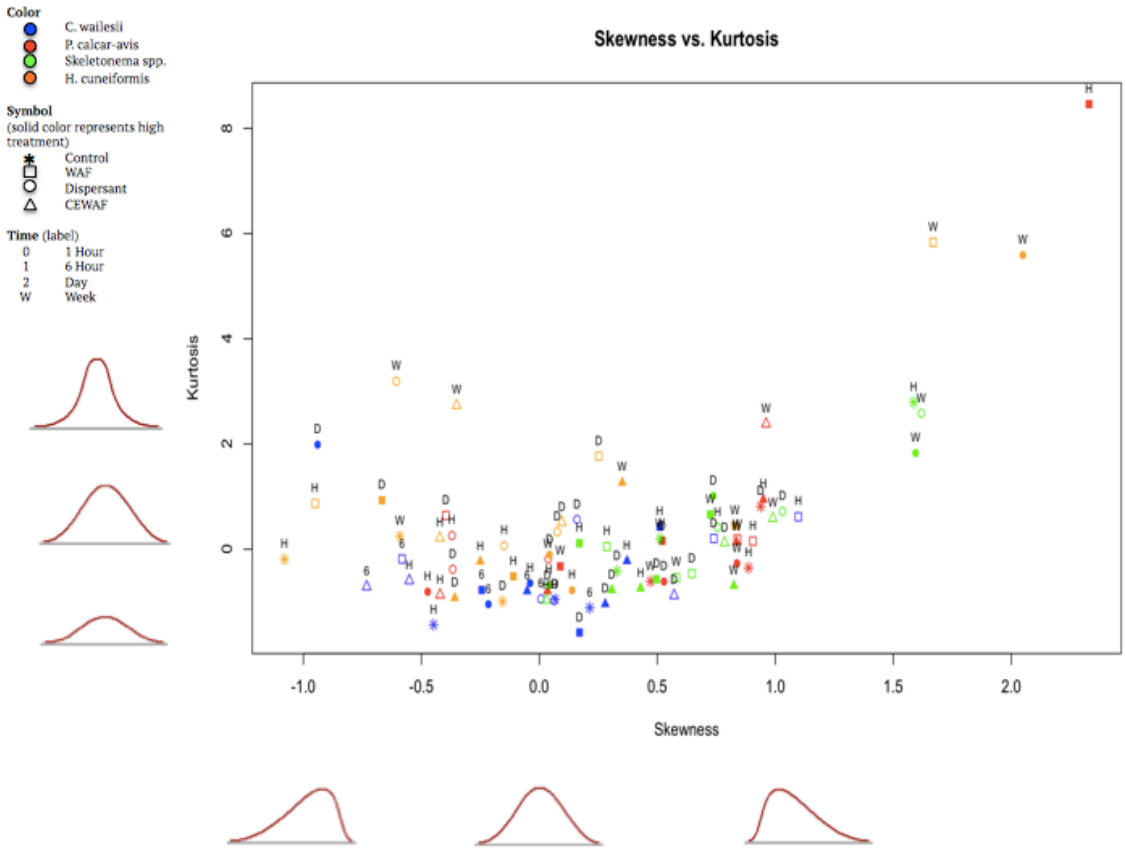

Figure 22: A bi-plot of Skewness vs. Kurtosis with all treatments. The Kurtosis represents the peak intensity of the distribution while the skewness is the lack of symmetry in either direction. Higher kurtosis values represent a stronger peak, while higher skewness represents increasing skew to the left.

References

Adams CM, Hernandez E, Cato JC. 2004. The economic significance of the Gulf of Mexico related to population, income, employment, minerals, fisheries and shipping. Ocean Coast Manage. 47(11):565–580.

Anderson L, Sweeney B. 1977. Diel changes in the sedimentation characteristics of *Ditylum brightwelli*, a marine centric diatom: changes in cellular lipids and effects of respiratory inhibitors and ion-transport modifiers. Limnol Oceanogr. 22(3):539-552.

Armbrust EV. 2009. The life of diatoms in the world's oceans. Nature. 459(7244):185–192.

Aurand, D., Coelho, G. 2005. (Ecosystem Management & Associates, Inc., Lusby, MD) Cooperative Aquatic Toxicity Testing of Dispersed Oil and the "Chemical Response to Oil Spills: Ecological Effects Research Forum (CROSERF)." Technical Report 07-03.

Behrenfeld MJ, Falkowski PG. 1997. Photosynthetic rates derived from satellite-based chlorophyll concentration. Limnol Oceanogr. 42(1):1-20.

Bienfang PK. 1980. Phytoplankton sinking rates in oligotrophic waters off Hawaii, USA. Mar Biol. 61(1):69–77.

Bienfang PK. 1981. SETCOL—a technologically simple and reliable method for measuring phytoplankton sinking rates. Can J Fish Aquat Sci. 38(10):1289-1294.

Bienfang PK, Harrison PJ. 1984. Sinking-rate response of natural assemblages of temperate and subtropical phytoplankton to nutrient depletion. Mar Biol. 83(3):293–300.

Bienfang, PK, Harrison PJ, Quarmby L. 1982. Sinking rate response to depletion of nitrate, phosphate and silicate in four marine diatoms. Mar Biol. 67(3):295-302.

Bienfang, PK, Szyper J, Laws E. 1983. Sinking rate and pigment responses to light-limitation of a marine diatom: implications to dynamics of chlorophyll maximum layers. Oceanol Acta. 6(1):55-62.

Brenner, H. 1962. Effect of finite boundaries on the Stokes resistance of an arbitrary particle. J Fluid Mech. 28(2):391–411.

Burrell D. 1988. Carbon flow in fjords. Oceanogr Mar Biol Annu Rev. 26(1):143-226.

Crone T, Tolstoy M. 2010. Magnitude of the 2010 Gulf of Mexico oil leak. Science. 330(6004): 634.

Culver M, Smith W. 1989. The effects of environmental variation on the sinking rates of marine phytoplankton. J Phycol. 25(2):262-270.

De la Huz R, Lastra M, Junoy J, Castellanos C, Vieitez JM. 2005. Biological impacts of oil pollution and cleaning in the intertidal zone of exposed sandy beaches: Preliminary study of the "Prestige" oil spill. Estuar Coast Shelf S. 65(1-2):19–29.

Dunstan, WM, Atkinson, LP, Natoli J. 1975. Stimulation and inhibition of phytoplankton growth by low molecular weight hydrocarbons. Mar Biol. 31(4):305–310.

Eppley RW, Holmes RW, Strickland J. 1967. Sinking rates of marine phytoplankton measured with a fluorometer. J Exp Mar Biol Ecol. 1(2):191–208.

Falkowski, PG, Raven JA. 2007. 2nd ed. Aquatic photosynthesis. Princeton (NJ): Princeton University Press.

Fisher N, Wente M. The release of trace elements by dying marine phytoplankton. Deep-Sea Res Pt I. 40(4):671-694.

Gavis J. 1976. Munk and Riley revisited: nutrient diffusion transport and rates of phytoplankton growth. J Mar Res. 34:161-179.

Gemmell B, Oh G, Villareal TA, Buskey E. Forthcoming 2016. Dynamic sinking behavior in marine phytoplankton: rapid changes in buoyancy may aid in nutrient uptake.

Gilde K, Pinckney J. 2012. Sublethal effects of crude oil on the community structure of estuarine phytoplankton. Estuaries Coasts. 35(3):853–861.

González J, Figueiras FG, Aranguren-Gassis M, Crespo BG, Fernández E, Morán XAG, Nieto-Cid M. 2009. Effect of a simulated oil spill on natural assemblages of marine phytoplankton enclosed in microcosms. Estuar Coast Shelf S. 83(3):265–276.

Gordon, DC, Prouse NJ. 1973. The effects of three oils on marine phytoplankton photosynthesis. Mar Biol. 22(4):329-333.

Granata T. 1991. Diel periodicity in growth and sinking rates of the centric diatom *Coscinodiscus concinnus*. Limnol Oceanogr. 36(1):132-l39.

Gross F, Zeuthen E. 1948. The buoyancy of plankton diatoms: a problem of cell physiology. Proc R Soc Lond B Bio. 135(880):382-389.

Harrison P, Cochlan W, Acreman J, Parsons T, Thompson P, Dovey H, Xiaolin C. 1986. The effects of crude oil and Corexit 9527 on marine phytoplankton in an experimental enclosure. Mar Environ Res. 18(2):93-109.

Hill DF. 2002. General density gradients in general domains: The “two-tank” method revisited. Exp Fluids. 32(4):434–440.

Hook S, Osborn H. 2012. Comparison of toxicity and transcriptomic profiles in a diatom exposed to oil, dispersants, dispersed oil. Aquat Toxicol. 124-125:139-151.

Hopkinson B, Dupont C, Allen A, Morel F. 2011. Efficiency of the CO_2-concentrating mechanism of diatoms. P Natl Acad Sci-Biol. 108(10):3830-3837.

Hsiao S, Kittle D, Foy M. 1978. Effects of crude oils and the oil dispersant Corexit on primary production of arctic marine phytoplankton and seaweed. Environ Pollut. 15(3):209-221.

Hu C, Weisberg RH, Liu Y, Zheng L, Daly KL, English DC, Zhao J, Vargo GA. 2011. Did the northeastern Gulf of Mexico become greener after the Deepwater Horizon oil spill? Geophys Res Lett. 38(9): L09601.

Huang YJ, Jiang ZB, Zeng JN, Chen QZ, Zhao YQ, Liao YB, Shou L, Xu XQ. 2011. The chronic effects of oil pollution on marine phytoplankton in a subtropical bay, China. Environ Monit Assess. 176(1-4):517–530.

Jackson G. 2005. Coagulation theory and models of oceanic plankton aggregation. In: Droppo I, Leppard G, Liss S, Milligan T, editor. Flocculation in natural and engineered environmental systems. Boca Raton (FL): CRC Press. p. 271–292.

Johnson T, Smith W. 1986. Sinking rates of phytoplankton assemblages in the Weddell Sea marginal ice zone. Mar Ecol Prog Ser. 33:131-137.

Judson R, Martin M, Reif D, Houck K, Knudsen T, Rotroff D, Xia M, Sakamuru S, Huang R, Shinn P, Austin C, Kavlock R, Dix D. 2010. Analysis of eight oil spill dispersants using rapid, in vitro tests for endocrine and other biological activity. Environ Sci Technol 44(15):5979–5985.

Jung SW, Oh Y, Joo C, Kang J, Kim M. 2012. Stronger impact of dispersant plus crude oil on natural phytoplankton assemblages in short-term marine mesocosms. J Hazard Mater. 217-218:338-349.

Kooistra WHCF, Gersonde R, Medlin LK, Mann DG. 2007. The Origin and evolution of the diatoms: Their adaptation to a planktonic existence. In: Falkowski PG, Knoll AH, editor. Evolution of primary producers in the sea. Burlington (MA): Elsevier. p. 207–249.

Kusk K. 1978. Effects of crude oil and aromatic hydrocarbons on the photosynthesis of the diatom *Nitzschia palea*. Physiol Plantarum. 43(1):1-6.

Lee R, Takahasi M, Beers J, Thomas W, Seibert D, Koeller P, Green D. 1977. Controlled ecosystems: Their use in the study of the effects of petroleum hydrocarbons on plankton. In: Vernberg F, Calabrese A, Thurburg, Vernberg W, editor. Physiological responses of marine biota to pollutants. New York (NY): Academic Press. p. 323-341.

Liu N, Xiong D, Gao H, Liu W, Gong WM, Liu K. 2006. Study on acute toxicity of three fuel oil to marine chlorella. Mar Environ Sci. 25:29–32.

Margalef R. 1978. Life forms of phytoplankton as survival alternatives in an unstable environment. Oceanol Act. 1(4):493-509.

McGenity, TJ, Folwell, BD, McKew BA, Sanni GO. 2012. Marine crude-oil biodegradation: a central role for interspecies interactions. Aquat Biosyst. 8(1):1-19.

Miklasz K, Denny M. 2010. Diatom sinking speeds: Improved prediction and insight from a modified Stokes' law. Limnol Oceanogr. 55(6):2513-2525.

Morgan AD, Shaw-Brown K, Bellingham I, Lewis A, Pearce M, Pendoley KL. 2014. Global oil spills and oiled wildlife response effort: Implications for oil spill contingency planning. International Oil Spill Conference Proceedings; 2014 May 5-8; Savannah, GA.

Munk WH, Riley GA. 1952. Absorption of nutrients by aquatic plants. J Mar Res. 11:215-240.

Nelson-Smith A. 1973. 1st ed. Oil pollution and marine ecology. London: Elek.

O'Brien K, Waite A, Alexander B, Perry K, Neumann L. 2006. Particle tracking in a salinity gradient: A method for measuring sinking rate of individual phytoplankton in the laboratory. Limnol Oceanogr-Meth. 4(9):329-335.

Oil Budget Calculator Science and Engineering Team (U.S.). 2010. Oil budget calculator: Deepwater Horizon. [Washington, D.C.]: Federal Interagency Solutions Group, Oil Budget Calculator Science and Engineering Team.

Ozhan K, Bargu S. 2014a. Can crude oil toxicity on phytoplankton be predicted based on toxicity data on Benzo(a)Pyrene and Naphthalene? Bull Environ Contam Toxicol. 92(2):225–230.

Ozhan K, Bargu S. 2014b. Distinct responses of Gulf of Mexico phytoplankton communities to crude oil and the dispersant Corexit EC9500A under different nutrient regimes. Ecotoxicology. 23(3):370-384.

Ozhan K, Parsons ML, Bargu S. 2014a. How were phytoplankton affected by the Deepwater Horizon oil spill? Bioscience. 64(9):829–836.

Ozhan K, Miles SM, Gao H. 2014b. Relative phytoplankton growth responses to physically and chemically dispersed South Louisiana sweet crude oil. Environ Monit Assess. 186(6):3941–3956.

Parsons T, Harrison P, Acreman J, Dovey H, Thompson P, Lalli C. 1984. An experimental marine ecosystem response to crude oil and Corexit 9527: Part 2-Biological effects. Mar Environ Res. 13(4):265-275.

Parsons T, Li W, Waters R. 1976. Some preliminary observations on the enhancement of phytoplankton growth by low levels of mineral hydrocarbons. Hydrobiologia. 51(1):85-89.

Passow U. 2000. Formation of transparent exopolymer particles, TEP, from dissolved precursor material. Mar Ecol Prog Ser. 192:1–11.

Passow U, Ziervogel K, Asper V, Diercks A. 2012. Marine snow formation in the aftermath of the Deepwater Horizon oil spill in the Gulf of Mexico. Environ Res Lett. 7(3):1-11.

Patton J, Rigler M, Boehm P, Fiest D. 1981. Ixtoc 1 oil spill: flaking of surface mousse in the Gulf of Mexico. Nature. 290(5803):235–8.

Pulich WM, Winters K, Baalen CV. 1974. The effects of a No. 2 fuel oil and two crude oils on the growth and photosynthesis of microalgae. Mar Biol. 28(2):87–94.

Ragueneau O, Tréguer P, Leynaert A, R Anderson, Brzezinski M, DeMaster D, Dugdale R, Dymond J, Fischer G, François R, Heinze C, Reimer E, Martin-Jézéquel V, Nelson D, Quéguiner B. 2000. A review of the Si cycle in the modern ocean: recent progress and missing gaps in the application of the biogenic opal as a paleoproductivity proxy. Global Planet Change. 26(4):317-265.

Ruiz J, Macías D, Peters F. 2004. Turbulence increases the average settling velocity of phytoplankton cells. P Natl Acad Sci USA. 101(51):17720–17724.

Sbalzarini I, Koumoutsakos P. 2005. Feature point tracking and trajectory analysis for video imaging in cell biology. J Struct Biol. 151(2):182-195.

Schöne H, Schöne A. 1982. MET 44: A weakly enriched sea-water medium for ecological studies on marine plankton algae, and some examples of its application. Bot Mar. 25(3):117-122.

Sikkema J, de Bont JA, Poolman B. 1995. Mechanisms of membrane toxicity of hydrocarbons. Microbiol Rev. 59(2):201–222.

Smayda TJ. 1970. The suspension and sinking of phytoplankton in the sea. Oceanogr Mar Biol. 8:353-414.

Smayda TJ. 1971. Normal and accelerated sinking of phytoplankton in the sea. Mar Geol. 11(2):105-122.

Smayda TJ. 1974. Some experiments on the sinking characteristics of two freshwater diatoms. Limnol Oceanogr. 19(4):628–635.

Smayda TJ, Boleyn B. 1965. Experimental observations on the flotation of marine diatoms. *I. Thalassiosira cf. nana, Thalassiosira rotula*, and *Nitzschia seriata*. Limnol Oceanogr. 10(4):449-509.

Smayda TJ, Boleyn B. 1966. Experimental observations on the flotation of marine diatoms. *II. Skeletonema costatum* and *Rhizosolenia setigera.* Limnol Oceanogr. 11(1):18-34.

Smayda TJ, Reynolds CJ. 2001. Community assembly in marine phytoplankton: application of recent models to harmful dinoflagellate blooms. J Plankton Res. 23(5):447-461.

Smetacek V. 1985. Role of sinking in diatom life history cycles: ecological, evolutionary, and geological significance. Mar Biol. 84(3):239-251.

Villareal TA. 1991. Buoyancy properties of the giant diatom *Ethmodiscus*. J Plankton Res. 14(3):459-463.

Villareal TA, Carpenter E. 1990. Diel buoyancy regulation in the marine diazotrophic cyanobacterium *Trichodesmium thiebautii*. Limnol Oceanogr. 35(8):1832-1837.

Villareal TA, Carpenter E. 2003. Buoyancy regulation and the potential for vertical migration in the oceanic cyanobacterium *Trichodesmium*. Microb Ecol. 45(1):1-10.

Waite A, Thompson P, Harrison P. 1992. Does energy control the sinking rate of marine diatoms? Limnol Oceanogr. 37(3):468-477.

Waite A, Fisher A, Thompson P, Harrison P. 1997. Sinking rate versus cell volume relationships illuminate sinking rate control mechanisms in marine diatoms. Mar Ecol Prog Ser. 157:97–108.

Walsby A, Holland D. 2006. Sinking velocities of phytoplankton measured on a stable density gradient by laser scanning. J Roy Soc Interface. 3(8):429-439.

Walsby AE, Reynolds CS. 1980. Sinking and floating. In: Morris I, editor. The physiological ecology of phytoplankton. Oxford: Blackwell Scientific Publications. p. 371-412.

Vita

Genesok Oh, the son of Seiwoong and Sunmi Oh, was born in Denton, Texas, and shortly after moved to Newtown, Pennsylvania. After graduating from Council Rock North High School in 2009, he attended Stony Brook University in Stony Brook, NY. Gene received his Bachelor of Science degree in Marine Science in May of 2013. In August of 2013, he entered the University of Texas at Austin as a graduate student in the department of Marine Science.

Permanent address: 17 Snapdragon Drive., Newtown, PA 18940

This thesis was typed by the author.